

NIST Technical Note 1760

Smoke Component Yields from Bench-Scale Fire Tests: 1. NFPA 269 / ASTM E 1678

Nathan D. Marsh
Richard G. Gann
Jason D. Averill
Marc R. Nyden

<http://dx.doi.org/10.6028/NIST.TN.1760>



NIST Technical Note 1760

Smoke Component Yields from Bench-Scale Fire Tests: 1. NFPA 269 / ASTM E 1678

Nathan D. Marsh

Richard G. Gann

Jason D. Averill

Marc R. Nyden

*Fire Research Division
Engineering Laboratory*

<http://dx.doi.org/10.6028/NIST.TN.1760>

December 2013



U.S. Department of Commerce
Penny Pritzker, Secretary

National Institute of Standards and Technology

Patrick D. Gallagher, Under Secretary of Commerce for Standards and Technology and Director

Certain commercial entities, equipment, or materials may be identified in this document in order to describe an experimental procedure or concept adequately. Such identification is not intended to imply recommendation or endorsement by the National Institute of Standards and Technology, nor is it intended to imply that the entities, materials, or equipment are necessarily the best available for the purpose.

National Institute of Standards and Technology Technical Note 1760
Natl. Inst. Stand. Technol. Tech. Note 1760, 57 pages (December 2013)
<http://dx.doi.org/10.6028/NIST.TN.1760>
CODEN: NTNOEF

ABSTRACT

A standard procedure is needed for obtaining smoke toxic potency data for use in fire hazard and risk analyses. Room fire testing of finished products is impractical, directing attention to the use of apparatus that can obtain the needed data quickly and at affordable cost. This report examines the first of a series bench-scale fire tests to produce data on the yields of toxic products in both pre-flashover and post-flashover flaming fires. The apparatus is the radiant furnace in NFPA 269 and ASTM E 1678. Test specimens were cut from finished products that were also burned in room-scale tests: a sofa made of upholstered cushions on a steel frame, particleboard bookcases with a laminated finish, and household electric power cable. Initially, the standard test procedure was followed, with a variation to reduce the contribution to the effluent of post-flaming pyrolysis. Subsequent variations in the procedure included cutting the test specimen into small pieces and performing the tests at a reduced oxygen volume fraction of 0.17. The yields of CO₂ CO, HCl, and HCN were determined. The yields of other toxicants (NO, NO₂, formaldehyde, and acrolein) were below the detection limits, but volume fractions at the detection limits were shown to be of limited toxicological importance relative to the detected toxicants. In general, dicing the test specimen and performing the tests at the reduced oxygen volume fraction had little effect on the toxic gas yields, within the experimental uncertainties. The exceptions were an increase in the CO yield for diced specimens at reduced oxygen, a decrease in the HCN yield from the intact sofa and cable specimens at reduced oxygen, and an increase in the HCN yield from dicing the cable specimens. In none of the procedure variations did the CO yield approach the value of 0.2 found in real-scale postflashover fire tests.

Keywords: fire, fire research, smoke, room fire tests, fire toxicity, smoke toxicity

This page intentionally left blank

TABLE OF CONTENTS

LIST OF FIGURES	VI
LIST OF TABLES.....	VI
I. INTRODUCTION.....	1
A. CONTEXT OF THE RESEARCH	1
B. OBTAINING INPUT DATA.....	2
C. PRIOR ROOM-SCALE TESTS.....	3
1. <i>Test Configuration</i>	3
2. <i>Combustibles</i>	4
3. <i>Test Conduct</i>	8
D. PHYSICAL FIRE MODELS	9
II. EXPERIMENTAL INFORMATION	11
A. SUMMARY OF NFPA 269/ASTM E 1678 APPARATUS.....	11
1. <i>Hardware</i>	11
2. <i>Gas Sampling and Analysis Systems</i>	15
B. OPERATING PROCEDURES	19
1. <i>"Standard" Testing</i>	19
2. <i>Test Specimens</i>	20
3. <i>Test Procedure Variation</i>	21
C. DATA COLLECTION.....	22
III. CALCULATION METHODS.....	23
A. NOMENCLATURE	23
B. MASS LOSS RATE.....	24
C. NOTIONAL GAS YIELDS	24
D. CALCULATED GAS YIELDS	25
1. <i>CO and CO₂</i>	25
2. <i>HCl</i>	27
3. <i>HCN</i>	27
4. <i>Other Gases</i>	28
IV. RESULTS.....	29
A. TESTS PERFORMED	29
B. CALCULATIONS OF TOXIC GAS YIELDS WITH UNCERTAINTIES	36
V. DISCUSSION	39
A. OVERALL TEST VALUES	39
B. SPECIMEN PERFORMANCE AND TEST REPEATABILITY	39
1. <i>CO₂ and CO</i>	39
2. <i>HCl and HCN</i>	45
C. MEASURED VS. NOTIONAL VALUES	46
D. SPECIES SAMPLING AND MEASUREMENT.....	46
1. <i>Species Measurement Using FTIR Spectroscopy</i>	46
2. <i>Chimney Sampling</i>	47
E. IMPORTANCE OF UNDETECTED GASES	48
VI. CONCLUSION	51
VII. ACKNOWLEDGMENTS	53
REFERENCES	55

LIST OF FIGURES

FIGURE 1. PHOTOGRAPH OF THE RADIANT TEST APPARATUS.....	11
FIGURE 2. SCHEMATIC OF THE RADIANT TEST APPARATUS	11
FIGURE 3. PHOTOGRAPH OF THE COMBUSTION CELL, SPECIMEN SUPPORT, RADIANT HEATERS, AND CHIMNEY.....	12
FIGURE 4. SCHEMATIC OF THE RADIANT FLUX DISTRIBUTION TEMPLATE.....	13
FIGURE 5. MEAN RADIANT FLUX VS. RADIANT HEATER POWER SETTING. ERROR BARS ARE THE STANDARD DEVIATION ACROSS THE DIFFERENT GAUGE POSITIONS.....	14
FIGURE 6. FTIR SPECTRUM OF THE PRODUCTS OF BURNING ELECTRICAL CABLE.....	18
FIGURE 7. PHOTOGRAPHS OF TEST SPECIMENS.....	22
FIGURE 8. CO ₂ VOLUME FRACTION VS. PEAK AREA.....	25
FIGURE 9. [φ _{CO} /φ _{CO₂}] _{CHAMBER} VS. [φ _{CO} /φ _{CO₂}] _{CHIMNEY}	26
FIGURE 10. RATIOS OF CO ₂ AND CO VOLUME FRACTIONS MEASURED USING NDIR AND FTIR SPECTROSCOPY VS. THE NDIR CO/CO ₂ VOLUME FRACTION RATIO.	29
FIGURE 11. GAS VOLUME FRACTIONS FROM FOUR BOOKCASE SPECIMEN TESTS. (SOLID, CO ₂ ; DOTTED, CO; DASHED, O ₂).	40
FIGURE 12. COMPARISON OF OXYGEN CONSUMPTION (TOP HALF OF FIGURE) AND CO ₂ PRODUCTION (BOTTOM HALF OF FIGURE) IN BOOKCASE SPECIMEN TESTS AT OXYGEN VOLUME FRACTIONS OF 0.21 (SOLID LINES) AND 0.17 (DOTTED LINES).....	41
FIGURE 13. COMPARISON OF CO PRODUCTION IN BOOKCASE SPECIMEN TESTS WITH OXYGEN VOLUME FRACTIONS OF 21 % (SOLID LINES) AND 17 % (DOTTED LINES). NOTE THE CHANGE OF ORDINATE SCALE AT MASS LOSS OF 50 %.	42
FIGURE 14. COMPARISON OF CO PRODUCTION IN BOOKCASE SPECIMEN TESTS IN SLAB (SOLID LINES) AND DICED (DOTTED LINES) CONFIGURATIONS. NOTE THE CHANGE OF ORDINATE SCALE AT MASS LOSS OF 50 PERCENT.	43
FIGURE 15. COMPARISON OF CO PRODUCTION IN ELECTRICAL CABLE TESTS IN WHOLE (SOLID LINES) AND DICED (DOTTED LINES) CONFIGURATIONS. NOTE THE CHANGE OF ORDINATE SCALE AT MASS LOSS OF 50 PERCENT.	44
FIGURE 16. COMPARISON OF OXYGEN CONSUMPTION (TOP HALF OF FIGURE) AND CO ₂ PRODUCTION (BOTTOM HALF OF FIGURE) IN SOFA SPECIMEN TESTS AT OXYGEN VOLUME FRACTIONS OF 0.21 (SOLID LINES) AND 0.17 (DOTTED LINES).....	45

LIST OF TABLES

TABLE 1. ELEMENTAL ANALYSIS OF FUELS.....	5
TABLE 2. ELEMENTAL ANALYSIS OF FUEL COMPONENTS.....	7
TABLE 3. HEATS OF COMBUSTION OF FUELS.....	7
TABLE 4. TYPICAL MEASURED RADIANT FLUX VALUES.....	13
TABLE 5. SPECIES AND FREQUENCY WINDOWS FOR FTIR ANALYSIS.....	19
TABLE 6. CALCULATED NOTIONAL YIELDS OF TOXIC PRODUCTS FROM THE TEST SPECIMENS.	24
TABLE 7. DATA FROM BOOKCASE MATERIAL TESTS.	30
TABLE 8. GAS YIELDS FROM BOOKCASE MATERIAL TESTS.	31
TABLE 9. DATA FROM SOFA MATERIAL TESTS.	32
TABLE 10. GAS YIELDS FROM SOFA MATERIAL TESTS.	33
TABLE 11. DATA FROM CABLE MATERIAL TESTS.	34
TABLE 12. GAS YIELDS FROM CABLE MATERIAL TESTS.	35
TABLE 13. YIELDS OF COMBUSTION PRODUCTS FROM RADIANT FURNACE TESTS.....	36
TABLE 14. FRACTIONS OF NOTIONAL YIELDS OF COMBUSTION PRODUCTS FROM RADIANT FURNACE TESTS.	37
TABLE 15. LIMITS OF IMPORTANCE OF UNDETECTED TOXICANTS.....	49

I. INTRODUCTION

A. Context of the Research

Estimation of the times that building occupants will have to escape, find a place of refuge, or survive in place in the event of a fire is a principal component in the fire hazard or risk assessment of a facility. An accurate assessment enables public officials and facility owners to provide a selected or mandated degree of fire safety with confidence. Without this confidence, regulators and/or designers tend to apply large safety factors to lengthen the tenable time. This can increase the cost in the form of additional fire protection measures and can eliminate the consideration of otherwise desirable facility designs and construction products. Error in the other direction is also risky, in that if the time estimates are incorrectly long, the consequences of a fire could be unexpectedly high.

Such fire safety assessments now rely on some form of computation that takes into account multiple, diverse factors, including the facility design, the capabilities of the occupants, the potential growth rate of a design fire, the spread rates of the heat and smoke, and the impact of the fire effluent (toxic gases, aerosols, and heat) on people who are in or moving through the fire vicinity.¹ The toolkit for these assessments, while still evolving, has achieved some degree of maturity and quality. The kit includes such tools as:

- Computer models of the movement and distribution of fire effluent throughout a facility.
 - Zone models, such as CFAST², have been in use for over two decades. This model takes little computational time, a benefit achieved by simplifying the air space in each room into two zones. A number of laboratory programs, validation studies³, and reconstructions of actual fires have given credence to the predictions.⁴
 - Computational fluid dynamics (CFD) models, such as the Fire Dynamics Simulator (FDS)⁵, have seen increased use over the past decade. FDS is more computationally intense than CFAST in order to provide three-dimensional temperature and species concentration profiles. There has been extensive verification and validation of FDS simulations.^{5,6}

These models calculate the local temperatures and combustion product concentrations as the fire develops. These profiles can be used for estimating when a person would die or be incapacitated, *i.e.*, is no longer able to effect his/her own escape.

- Devices such as the cone calorimeter⁷ and larger scale apparatus⁸, which are routinely used to generate information on the rate of heat release as a commercial product burns.
- A number of standards from ISO TC92 SC3 that provide support for the generation and use of fire effluent information in fire hazard and risk analyses.⁹ Of particular importance is ISO 13571, which provides consensus equations for estimating the human incapacitating exposures to the narcotic gases, irritant gases, heat, and smoke generated in fires.¹⁰

More problematic are the sources of data for the production of the harmful products of combustion. Different materials can generate fire effluent with a wide range of toxic potencies.

Most furnishing and interior finish products are composed of multiple materials assembled in a variety of geometries, and there is as of yet no methodology for predicting the evolved products from these complex assemblies. Furthermore, the generation of carbon monoxide (CO), the most common toxicant, can vary by orders of magnitudes, depending on the fire conditions.¹¹

An analysis of the U.S. fire fatality data¹² showed that post-flashover fires comprise the leading scenarios for life loss from smoke inhalation. Thus, it is most important to obtain data regarding the generation of harmful species under post-flashover (or otherwise underventilated) combustion conditions. Data for pre-flashover (well-ventilated) conditions have value for ascertaining the importance of prolonged exposure to "ordinary" fire effluent and to short exposures to effluent of high potency.

B. Obtaining Input Data

The universal metric for the generation of a toxic species from a burning specimen is the yield of that gas, defined as the mass of the species generated divided by the consumed mass of the specimen.¹³ If both the mass of the test specimen and the masses of the evolved species are measured continuously during a test, then it is possible to obtain the yields of the evolved species as the burning process, and any chemical change within the specimen, proceeds. If continuous measurements are not possible, there is still value in obtaining a yield for each species integrated over the burning history of the test specimen.

The concentrations of the gases (resulting from the yields and the prevalent dilution air) are combined using the equations in ISO 13571 for a base set of the most prevalent toxic species. Additional species may be needed to account for the toxic potency of the fire-generated environment.

To obtain an indicator of whether the base list of toxic species needs to be enhanced, living organisms should also be exposed to the fire effluent. The effluent exposure that generates an effect on the organisms is compared to the effect of exposure to mixtures of the principal toxic gases. Disagreement between the effluent exposure and the mixed gas exposure is an indicator of effluent components not included in the mixed gas data or the existence of synergisms or antagonisms among the effluent components. This procedure has been standardized, based on data developed using laboratory rats.^{14,15} However, it is recognized that animal testing is not always possible. In these cases, it is important to identify, from the material degradation chemistry, a reasonable list of the degradation and combustion products that might be harmful to people.

Typically, the overall effluent from a fire is determined by the large combustibles, such as a bed or a row of auditorium seats. The ideal fire test specimen for obtaining the yields of effluent components is the complete combustible item, with the test being conducted in an enclosure of appropriate size. Unfortunately, reliance on real-scale testing of commercial products is impractical, both for its expense per test and for the vast number of commercial products used in buildings. Such testing *is* practical for forensic investigations in which there is knowledge of the specific items that combusted.

A more feasible approach for obtaining toxic gas yields for facility design involves the use of a physical fire model – a small-scale combustor that captures the essence of the combustible and of the burning environment of interest. The test specimen is an appropriate cutting from the full combustible. To have confidence in the accuracy of the effluent yields from this physical fire model, it must be demonstrated:

- How to obtain, from the full combustible, a representative cutting that can be accommodated and burned in the physical fire model;
- That the combustion conditions in the combustor (with the test specimen in place) are related to the combustion conditions in the fire of interest, generally pre-flashover flaming (well ventilated or underventilated), post-flashover flaming, pyrolysis, or smoldering;
- How well, for a diverse set of combustible items, the yields from the small-scale combustor relate to the yields from real-scale burning of the full combustible items; and
- How sensitive the effluent yields are to the combustor conditions and to the manner in which the test specimen was obtained from the actual combustible item.

At some point, there will be sufficient data to imbue confidence that testing of further combustibles in a particular physical fire model will generate yields of effluent components with a consistent degree of accuracy.

The National Institute of Standards and Technology (NIST) has completed a project to establish a technically sound protocol for assessing the accuracy of bench-scale device(s) for use in generating fire effluent yield data for fire hazard and risk evaluation. In this protocol, the yields of harmful effluent components are determined for the real-scale burning of complete finished products during both pre-flashover and post-flashover conditions. Specimens cut from these products are then burned in various types of bench-scale combustors using their standard test protocols. The test protocols are then varied within the range of the combustion conditions related to these fire stages to determine the sensitivity of the test results to the test conditions and to provide a basis for improving the degree of agreement with the yields from the room-scale tests.

This report continues with a brief description of the previously conducted room fire tests. The full details can be found in Reference 16. Following this recap are the details of the tests using the first of four bench-scale apparatus to be examined.

C. Prior Room-scale Tests

1. Test Configuration

With additional support from the Fire Protection Research Foundation, NIST staff conducted a series of room-fire tests of three complex products [16]. The burn room was 2.44 m wide, 2.44 m high, and 3.66 m long (8 ft x 8 ft x 12 ft). The attached corridor was a 9.75 m (32 ft) long

extension of the burn room. A doorway 0.76 m (30 in.) wide and 2.0 m (80 in.) high was centered in the common wall. The downstream end of the corridor was fully open.

2. Combustibles

Three fuels were selected for diversity of physical form, combustion behavior, and the nature and yields of toxicants produced. Supplies of each of the test fuels were stored for future use in bench-scale test method assessment.

- “Sofas” made of up to 14 upholstered cushions supported by a steel frame. The cushions consisted of a zippered cotton-polyester fabric over a block of a flexible polyurethane (FPU) foam. The fire retardant in the cushion padding contains chlorine atoms. Thus, this fuel would be a source of CO₂, CO, HCN, HCl, and partially combusted organics. The ignition source was the California TB133 propane ignition burner¹⁷ faced downward, centered over the center of the row of seat cushions. In all but two of the tests, the sofa was centered along the rear wall of the burn room facing the doorway. In the other two tests, the sofa was placed in the middle of the room facing away from the doorway to compare the burning behavior under different air flow conditions. Two of the first group of sofa tests were conducted in a closed room to examine the effect of vitiation on fire effluent generation. In these, an electric “match” was used to initiate the fires.
- Particleboard (ground wood with a urea formaldehyde binder) bookcases with a laminated polyvinylchloride (PVC) finish. This fuel would be a source of CO₂, CO, partially combusted organics, HCN, and HCl. To sustain burning, two bookcases were placed in a “V” formation, with the TB133 burner faced upward under the lower shelves.
- Household wiring cable, consisting of two 14 gauge copper conductors insulated with a nylon and a polyvinyl chloride (PVC), an uninsulated ground conductor, two paper filler strips, and an outer cable jacket of a plasticized PVC. This fuel would be a source of CO₂, CO, HCl, and partially combusted organics. Two cable racks containing 3 trays each supported approximately 30 kg of cable in each of the bottom two trays and approximately 17 kg in each of the middle and top trays. The cable trays were placed parallel to the rear wall of the burn room. Twin propane ignition burners were centered under the bottom tray of each rack.

The elemental chemistry of each combustible was determined by an independent testing laboratory. The analytical chemical data are shown in Table 1. The elemental composition of the component materials in the fuels is shown in Table 2. Additional data on the heats of combustion (triplicate samples) are shown in Table 3.

The details of the composition of the fuels and their test configurations are discussed below. The ignition modes and test configurations were selected to provide burning durations (under both well-ventilated and ventilation-limited conditions) that were long enough for accurate combustion product analyses. In some cases, adherence to realism was sacrificed to achieve this. Some of the sofas were burned in two different orientations to estimate the effect of fuel location on combustion product yields.

Table 1. Elemental Analysis of Fuels.

Sample	Mass %														Δ^*	O**	Remainder
	C	H	N	Cl	Ca	Pb	Al	Sb	P	Sn	Ti	Total					
Particle Board, with laminate	46.89	6.70	2.68	0.26	n	n	n	n	n	n	n	56.53	43.47				
	46.56	6.68	3.35	0.24	n	n	n	n	n	n	n	56.83	43.17				
	47.12	6.60	2.76	0.26	n	n	n	n	n	n	n	56.74	43.26				
Mean value	46.86	6.66	2.93	0.25								56.70	43.30	42.6	0.7		
Standard deviation	0.28	0.05	0.37	0.01								0.15	0.15				
Pressboard, with laminate	43.04	6.12	0.21	0.14	n	n	n	n	n	n	n	49.51	50.49				
	43.12	6.08	0.21	0.15	n	n	n	n	n	n	n	49.56	50.44				
	42.73	6.20	0.18	0.14	n	n	n	n	n	n	n	49.25	50.75				
Mean value	42.96	6.13	0.20	0.14								49.44	50.56				
Standard deviation	0.21	0.06	0.02	0.01								0.17	0.17				
Cushion fabric	47.23	6.23	0.18	n	n	n	n	n	n	n	n	53.64	46.36				
	48.12	6.10	0.19	n	n	n	n	n	n	n	n	54.41	45.59				
	47.38	5.99	0.20	n	n	n	n	n	n	n	n	53.57	46.43				
Mean value	47.58	6.11	0.19									53.87	46.13	46.5	0.4		
Standard deviation	0.48	0.12	0.01									0.47	0.47				
Cushion padding	56.38	8.48	12.58	0.95	n	n	n	n	0.20	n	n	78.59	21.41				
	56.33	8.58	12.50	0.90	n	n	n	n	0.15	n	n	78.46	21.54				
	56.36	8.53	12.46	0.71	n	n	n	n	0.21	n	n	78.27	21.73				
Mean value	56.36	8.53	12.51	0.85					0.19			78.44	21.56	25	-3.5		
Standard deviation	0.03	0.05	0.06	0.13					0.03			0.16	0.16				
Cable jacket	40.83	5.07	<0.10	26.77	10.42	<0.05						72.67	27.33				
	40.94	5.20	<0.10	26.53	10.18	<0.05						72.67	27.33				
	40.87	5.15	<0.10	26.68	10.24	<0.05						72.70	27.30				
Mean value	40.88	5.14		26.66	10.28	<0.05						72.68	27.32	16.7	10.6		

Sample	Mass %														
	C	H	N	Cl	Ca	Pb	Al	Sb	P	Sn	Ti	Total	Δ *	O**	Remainder
Standard deviation	0.06	0.07		0.12	0.10							0.02	0.02		
Wire insulation	48.25	6.73	2.39	26.04			0.80	0.62				83.41	16.59		
	48.20	6.98	2.65	26.08			0.81	0.62				83.91	16.09		
	48.57	6.82	2.40	26.22			0.72	0.63				84.01	15.99		
Mean value	48.34	6.84	2.48	26.11			0.78	0.62				83.78	16.22	9.2	7.0
Standard deviation	0.20	0.13	0.15	0.09			0.04	0.00				0.32	0.32		
Cable filler	42.58	6.65	<0.10	n								49.23	50.77		
	42.42	6.84	<0.10	n								49.26	50.74		
	42.72	6.80	<0.10	n								49.52	50.48		
Mean value	42.57	6.76										49.34	50.66	38.4 (C) 49.0 (H)	
Standard deviation	0.15	0.10										0.16	0.16		
Cable residue	18.39	2.30	0.20	22.99								43.88	56.12		
				25.42											
	19.03	2.45	0.21	27.76								49.45	50.55		
				28.62											
	17.91	2.47	0.14	30.00								50.52	49.48		
				27.87											
Mean value	18.44	2.41	0.18	26.96								47.95	52.05		
Standard deviation	0.56	0.09	0.04	2.51								3.57	3.57		

* [1 - Σ (mass %) of listed elements]

** See following text for estimation methods

Table 2. Elemental Analysis of Fuel Components.

Sample	Mass %												
	C	H	N	Cl	Ca	Pb	Al	Sb	P	Sn	Ti	Ash	O
Wood	49.0	6.1	0.2									0.5	44
Paper	49.0	6.1	0.2									0.5	44
Urea formaldehyde	33.3	5.6	38.9										22.2
PVC	38.4	4.8		56.7									0
Diethyl phthalate	73.8	9.8											16.4
Melamine	28.6	4.8	66.7										0
Cotton (= cellulose)	44.5	6.2											49.3
Polyethylene terephthalate	62.5	4.2											33.3
Nylon 6,6	64	9.3	12										14
Nylon 6	66	10.2	11										13
FPU foam	57.6	5.6	11.2										25.6

Table 3. Heats of Combustion of Fuels.

Sample	ΔH_c (MJ/kg)			Mean	σ
Particle Board, with laminate	18.24	18.17	18.07	18.16	0.07
Pressboard, with laminate	16.48	16.18	16.26	16.31	0.03
Cushion fabric	18.17	17.96	17.94	18.02	0.10
Cushion padding	26.09	26.02	26.12	26.08	0.04
PVC sheet	16.67	16.48	1.27	16.47	0.17
Cable jacket	18.30	18.41	18.36	18.36	0.04
Wire insulation	23.39	23.33	23.45	23.39	0.06
Cable filler	17.01	17.00	17.00	17.00	0.00
Cable residue	Did not ignite				

The mass fractions of cover fabric and padding in the sofa cushions were determined to be 0.205 ± 0.004 and 0.795 ± 0.004 , respectively. Since the cushions appeared to burn evenly (*i.e.*, the fabric was generally not burned away well before the foam was) and since they were virtually consumed in the tests, we presumed that the elemental composition of the fuel was steady during the tests. We then estimated the cushion composition (mass fraction) to be:

C:	$0.545 \pm 1\%$
H:	$0.080 \pm 1\%$
N:	$0.100 \pm 1\%$
Cl:	$0.0068 \pm 16\%$
P:	$0.0015 \pm 17\%$
O:	$0.267 \pm 4\%$

The derived value for the heat of combustion for the cushions is $24.4 \text{ MJ/kg} \pm 3\%$. The mass density of the foam was measured as $0.031 \text{ g/cm}^3 \pm 6\%$; the areal density of the cover fabric was measured as $0.019 \text{ g/cm}^2 \pm 4\%$.

For the bookcases, we estimated the fuel composition (mass fraction) to be:

C:	$0.481 \pm 0.6\%$
H:	$0.062 \pm 0.8\%$
N:	$0.029 \pm 13\%$
Cl:	$0.0030 \pm 4\%$
O:	$0.426 \pm 1\%$

The heat of combustion for the bookcase is $18.2 \text{ MJ/kg} \pm 0.4\%$.

For the electric power cable, we measured the mass fractions of the insulation, filler paper, and jacket to be 0.516 ± 0.007 , 0.033 ± 0.0007 , and 0.239 ± 0.007 , respectively. The remainder of the mass was the copper wire. For the combustible material, the elemental composition was:

C:	$0.576 \pm 0.5\%$
H:	$0.080 \pm 1.5\%$
Cl:	$0.323 \pm 0.4\%$
N:	$0.021 \pm 6\%$

The heat of combustion for the combustible fraction of the cable is $21.60 \text{ MJ/kg} \pm 0.6\%$.

3. Test Conduct

During each test, the mass of each test specimen was monitored continuously. The concentrations of CO_2 , CO and O_2 were monitored in the burn room and at three locations in the corridor using species-specific analyzers. Fourier transform infrared (FTIR) spectroscopy was used to monitor CO_2 , CO , HCN , HCl , HF , HBr , NO , NO_2 , H_2CO (formaldehyde), and $\text{C}_3\text{H}_4\text{O}$

($\text{CH}_2=\text{CH}-\text{CH}=\text{O}$, acrolein) near the upstream and downstream ends of the corridor. Soot was measured gravimetrically near these two locations. All measurements were intended to be in the upper smoke layer. In the two tests with the doorway blocked, the effluent was sampled from the upper layer of the burn room.

For the open-door tests, the yields of the gases were determined by defining the pre- and post-flashover time intervals, determining the test specimen mass loss and the average volume fractions of the gases during those intervals, calculating the pre- and post-flashover yields of CO_2 from the above plus the calculated total mass flow through the doorway, and determining the yields of the other gases using the ratios of their mass fractions to the mass fraction of CO_2 .

For the closed-room tests, we assumed that the upper layer was well mixed. The measured volume fractions of the gases and the ideal gas law were used to calculate the mass of each species in the upper layer. These were normalized to specimen mass loss as a function of time.

The uncertainty in the yield values resulted from the sensitivity of the yield to the selected time pre- or post-flashover time interval, the uncertainty in the specimen mass loss, the uncertainty in the species mass flow out the doorway (for open door tests), and the quality of the assumptions inherent in the calculation of the mass of product in the upper layer (for closed room tests). For the closed room tests, the uncertainty was further estimated by comparing the yield values from the early combustion with those from the pre-flashover segments of the open door sofa tests. The analysis of similar tests also structured the determination of uncertainty and repeatability.

Many HCl and HCN measurements were close to the instrumental background. Nonetheless, the data were sufficient to obtain reasonable post-flashover yield values and pre-flashover yield estimates for the three combustibles. The post-flashover HCl and HCN concentrations were also high enough to obtain estimates of the degree of loss of the compounds down the length of the corridor. The pre-flashover values had too high a degree of uncertainty for this use.

The equations in ISO 13571 allow for additional gases to be included in estimating the time available for escape or refuge from a fire. The composition of the combustibles precluded the formation of some of these. Three key sensory irritants (NO_2 , acrolein, and formaldehyde) were not detected, thus establishing the upper limits of their presence. Analysis of these levels in light of their incapacitation concentrations from ISO 13571 showed they would have had less than a 20 % contribution to incapacitation relative to the concentration of HCl, except in the case of the bookcases, which produced little HCl. This unimportance of secondary toxicants is consistent with the results of the animal experiments used to establish the N-gas hypothesis that attributes fire effluent lethality to a small number of gases.¹⁸

D. Physical Fire Models

Historically, there have been numerous bench-scale devices that were intended for measuring the components of the combustion effluent.^{19,20} The combustion conditions and test specimen configuration in the devices vary widely, and some devices have flexibility in setting those conditions. Currently, ISO TC92 SC3 (Fire Threat to People and the Environment) is proceeding toward standardization of one of these devices, a tube furnace (ISO/TS 19700²¹) and is

considering standardization of another, the cone calorimeter (ISO 5660-1²²) with a controlled combustion environment. There are concurrent efforts in Europe and ISO to upgrade the chemical analytical capability for a closed box test (ISO 5659-2²³). Thus, before too long there may well be diverse (and perhaps conflicting) data on fire effluent component yields available for any given product. This situation does not support either assured fire safety or marketplace stability.

Only one device, used in both NFPA 269¹⁴ and ASTM E1678¹⁵, has been validated with animal exposure and gas measurement data against real-scale fire test data for the same materials, and then only for post-flashover yields of the principal toxicants.²⁴ The three, relatively homogeneous materials were Douglas fir, a rigid polyurethane foam, and an unplasticized PVC. The toxicology of the combustion products varied significantly among the three materials. Laboratory rats were exposed to the combustion effluent for 30 min and then observed for 14 days. The times of any animal deaths were recorded. The yields of the principal toxicants were also determined.

The validation was conducted according to five hypotheses:

1. The equal LC₅₀ hypothesis: LC₅₀ valuesⁱ, as measured in the bench-scale test and in the real scale, agree to within the acceptable uncertainty.
2. The primary toxic gas hypothesis: The bench-scale test shows the same primary toxic gases as the real-scale test.
3. The equal yields hypothesis: The yields of the measured toxic gases are the same, to within the acceptable uncertainty, in the bench-scale and in the real-scale tests.
4. The N-Gas hypothesis: The real-scale and the bench-scale results agree, to with the acceptable uncertainty, with predictions based on measured gas concentration and computations made according to the N-Gas Model.ⁱⁱ
5. The type-of-death hypothesis: The type of death (within- or post-exposure) is similar for the bench-scale and for the real-scale tests.

The agreement between the bench-scale results and the real-scale results was deemed to be within a factor of three, based on the hypothesis with the *worst* agreement. The LC₅₀ values agreed within approximately ± 50 %.

The existence of this prior validation suggested that this apparatus was a reasonable starting point for the current project. Accordingly, the apparatus was evaluated for specimens of the same batches of the finished *product* used in the previously reported room-fire tests.¹⁶ These combustibles were non-homogeneous and more complex than the three, relatively homogeneous materials previously used to estimate the validity of NFPA 269 and ASTM E 1678.

ⁱ The LC₅₀ is the concentration of a species that leads to the death of half (50 %) of the test animals within a specified time interval. An analogous metric is the IC₅₀ where the observed response is incapacitation.

ⁱⁱ When polymeric materials are thermally decomposed and burned, there are hundreds of species in the effluent. The N-Gas model postulates that the toxic potency of the effluent can be substantially explained using a small number, N, of these species. Typically, N is fewer than 10.

II. EXPERIMENTAL INFORMATION

A. Summary of NFPA 269/ASTM E 1678 Apparatus

1. Hardware

The apparatus consists of a radiant combustion cell, a collection chamber for the combustion effluent, and a chimney connecting the two. Figure 1 is a photograph of the apparatus, Figure 3 is a schematic of the apparatus, and Figure 3 depicts the combustion cell and radiant heaters; more detailed diagrams are in the NFPA and ASTM Standards. A brief description of the three components follows.

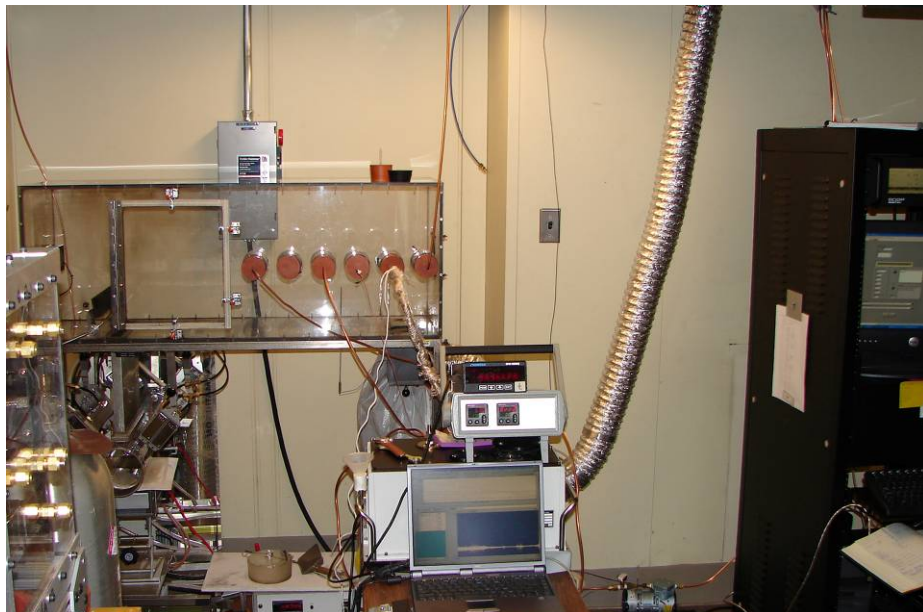


Figure 1. Photograph of the Radiant Test Apparatus.

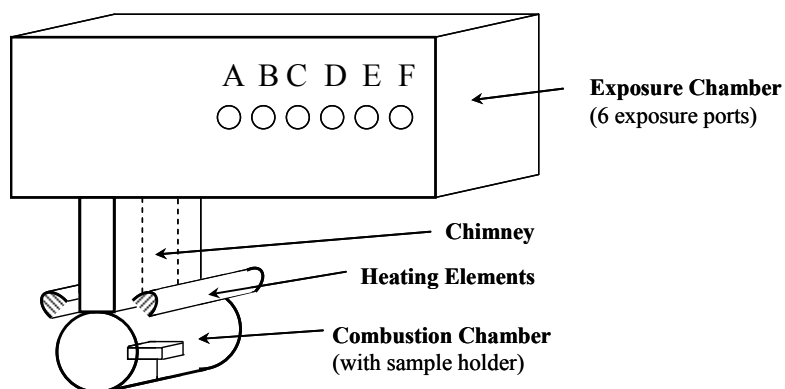


Figure 2. Schematic of the Radiant Test Apparatus

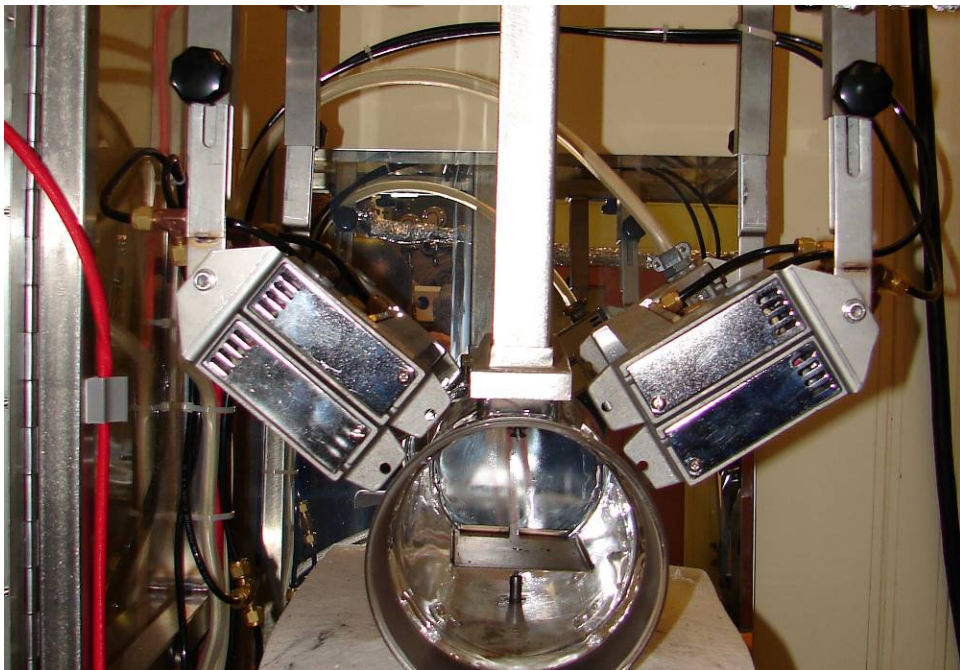


Figure 3. Photograph of the Combustion Cell, Specimen Support, Radiant Heaters, and Chimney.

a. Combustion Cell

The combustion cell is fabricated from a quartz ground glass joint, approximately 0.3 m long and 0.13 m in inner diameter. Within the cell is a platform upon which sits a tray containing the test specimen. A load cell sits below the combustion cell and is connected to the specimen tray by a solid rod. The load cell has a capacity of 500 g, with a rated resolution of 0.1 g. Electrodes are located within the cell to enable spark ignition of the specimen pyrolyzate.

Two quartz heaters, whose axes are parallel to the length of the combustion cell, apply radiant energy to the test specimen. According to the standard test procedures in the Standards, the orientation of the radiant heat lamps is to be adjusted so that no measurement at seven locations across the face of the specimen deviates more than 10 % from the average. Figure 4 depicts the steel template used to determine the radiant flux distribution. The template is made of steel sheet stock, with dimensions 8 cm x 13 cm x 5 cm high. The eight holes are approximately 1.4 cm in diameter.

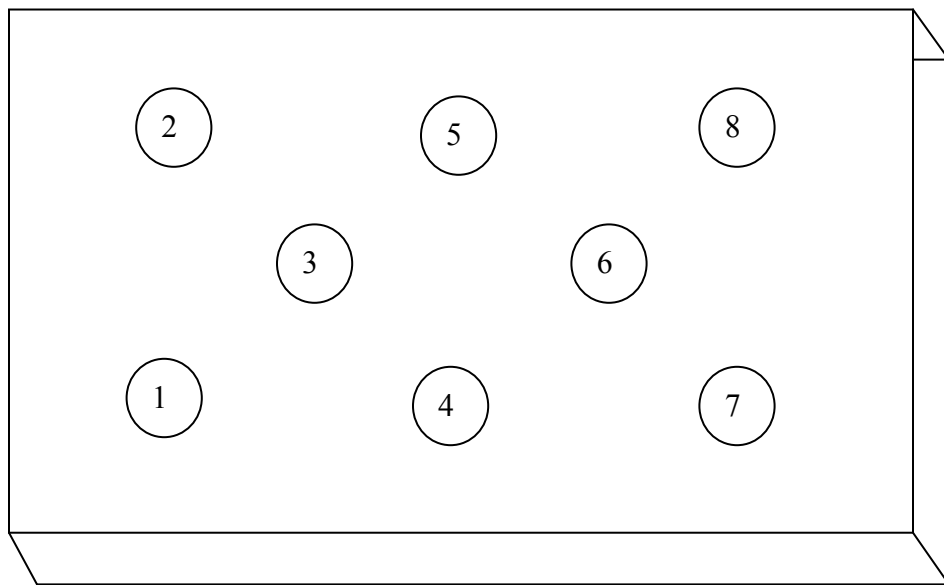


Figure 4. Schematic of the Radiant Flux Distribution Template.

The following procedure was used to determine the magnitude and uniformity of the radiant flux imposed on the test specimen for a given electrical power supplied to the heaters. The template was placed on the specimen platform and a Schmidt-Boelter heat flux gauge was inserted into the template such that its top surface was flush with the top surface of the template. A power setting for the radiant heaters was selected, and the heaters were allowed to stabilize for approximately five minutes. The electrical output of the gauge was recorded and converted to a radiant flux using the calibration curve supplied by the manufacturer. The gauge was then moved to each of the other holes in the template and the heat flux value recorded. The orientations of the heaters were then adjusted such that all measurements were within 10 % of the mean value, as required in the standards. One set of values is shown in Table 4. All are within the required interval except for the low value at Position 1 for the power setting of 250, and the high Position 2 value (at 350), both of which deviate by approximately 2 kW/m^2 . These are insignificant in the overall radiant flux to the test specimen, approximately no more than a 5 % flux reduction over approximately one-eighth of the surface. Figure 5 is a plot of these mean radiant flux values as a function of the dial setting on the heater power source.

Table 4. Typical Measured Radiant Flux Values.

Input Power Setting	Radiant Flux (kW/m^2)								
	Gauge Position								
	1	2	3	4	5	6	7	8	Mean
100	13	13	15	13	14	14	12	13	13.4
250	35	44	45	37	43	44	38	40	40.8
350	58	70	62	56	68	64	57	60	61.8

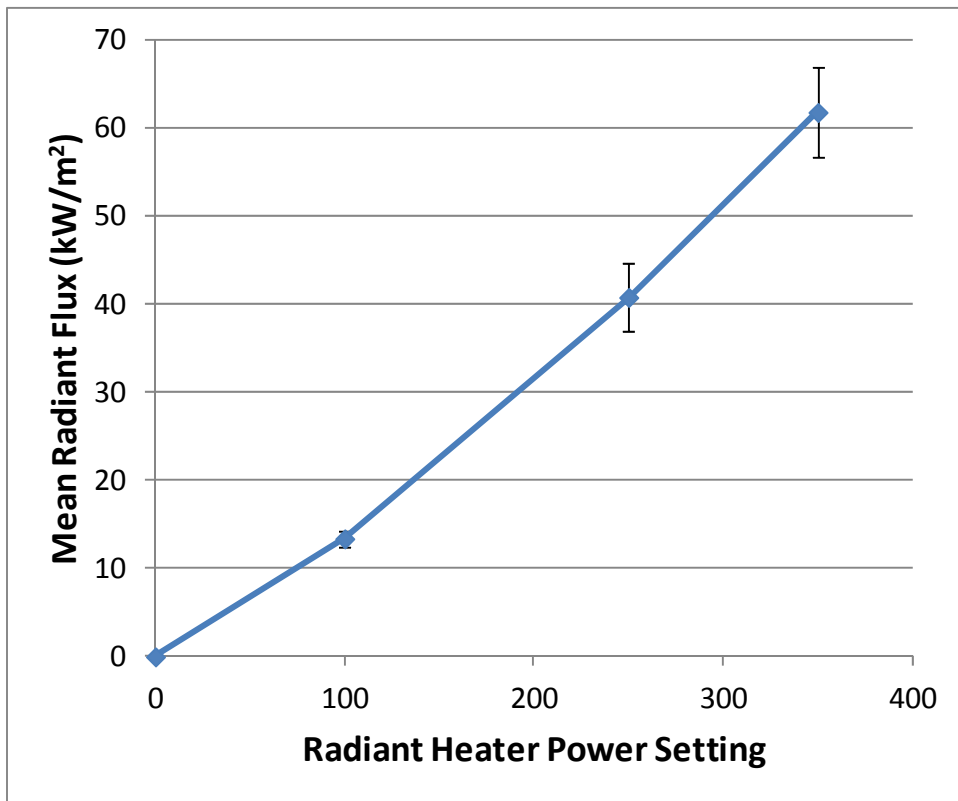


Figure 5. Mean Radiant Flux vs. Radiant Heater Power Setting. Error bars are the standard deviation across the different gauge positions.

All of the tests reported here were conducted at an irradiance of nominally $50 \text{ kW}/\text{m}^2$. Over time, the heaters aged and the radiant flux for a given power setting changed. The output of the heaters was checked periodically, and the appropriate power setting was selected.

b. Collection Chamber

The effluent collection chamber was fabricated of clear polycarbonate with inside dimensions of 1.22 m wide x 0.45 m deep x 0.37 m high, for a nominal volume of 0.2 m^3 . Across the front of the chamber are six ports, each nominally 63 mm inner diameter and 100 mm in length. They will be referred to as Ports A through F, from left to right in the figures above. In the standards, these are intended for supporting housings for the rats that would be exposed to the combustion effluent. In the tests reported here, the ports were closed with rubber stoppers. Four of the stoppers were penetrated by 6.25 mm outer diameter copper tubing. These were gas sampling and return lines for the fixed gas (CO , CO_2 , and O_2) analyzers and a Fourier transform infrared (FTIR) analyzer. Toward the left end of the chamber floor is a rectangular hole to the chimney, through which gas flowed to and from the combustion cell. A hinged lid to cap the chimney is operable from outside the chamber. On the right side of the floor of the chamber is a small fan to minimize any stratification of the combustion effluent within the chamber. Also on the right side of the chamber is a port for a plastic expansion bag. As warm combustion effluent enters the

chamber, the gas temperature in the chamber rises and the expansion bag inflates, minimizing any pressure increase in the chamber. This temperature rise did not exceed approximately 10 %.

c. Chimney

The 0.3 m tall chimney consists of three rectangular channels. The center channel (nominally 150 mm x 30 mm internal dimension) is centered over the test specimen. During a test, the combustion effluent rises through this center channel into the collection chamber. Flanking the center channel are two channels, each of whose internal cross section is nominally 70 mm x 30 mm. During a test, gas from the collection chamber flows downward through these channels to the burning specimen. The chimney is sealed to the combustion cell and to the collection chamber to minimize gas leakage during a test.

2. Gas Sampling and Analysis Systems

In the room-scale tests (Section I.C), measurements were made of 12 gases. Water and methane were included because of their potential interference with the quantification of the toxic gases. Two of the toxic gases, HBr and HF, were not found in the combustion products because there was no fluorine or bromine in the test specimens. The remaining eight toxic gases were acrolein (C_3H_4O), Carbon monoxide (CO), carbon dioxide (CO_2), formaldehyde (CH_2O), hydrogen chloride (HCl), hydrogen cyanide (HCN), nitric oxide (NO), and nitrogen dioxide (NO_2). Some of these turned out to be generated at levels that would not have contributed significantly to the incapacitation of exposed people. Thus, it was deemed unlikely that animal tests would have added much tenability information. As a result, the same gases were monitored in the bench-scale tests, and no animals were exposed. The basis for comparison between tests of the same combustibles at the two scales is the yields of the chemically diverse set of toxicants.

CO and CO_2 were quantified using a nondispersive infrared (NDIR) gas analyzer; oxygen was quantified by a paramagnetic analyzer in the same instrument. The precisions of the analyzers, as provided by the manufacturer, were:

CO: 10 $\mu L/L$

CO_2 : 0.02 L/L

O_2 : 0.05 L/L

For sampling from the collection chamber, gas was continuously drawn from Port C of the collection chamber through copper tubing of 6.35 mm outer diameter. The flow passed through a coiled tube immersed in a water ice bath; an impinger bottle immersed in dry ice, with its upper half filled with glass wool; and finally a glass fiber disk filter before reaching the pump and being returned to the chamber through Port F. The traps and filter removed particulates and condensable species, including water, that would otherwise interfere with and possibly harm the analyzer. The return minimized the effect of gas removal on the contents of the chamber. While sampling, the flow was maintained at 1 L/min for the CO and CO_2 detectors and 0.2 L/min for the O_2 detector. The analyzer itself was calibrated daily with zero and span gases (a mixture of 5000 $\mu L/L$ CO and 0.08 L/L of CO_2 in nitrogen, and ambient air (0.2095 L/L oxygen on a dry basis)). The span gas is certified to be accurate to within 2 % of the value.

The concentrations of CO, CO₂, and the additional six toxic gases were measured using a Midac Fourier transform infrared (FTIR) spectrometerⁱⁱⁱ equipped with a stainless steel flow cell (2 mm thick KBr windows and a 11.5 cm optical pathlength), maintained at (170 ± 5) °C. Samples were drawn through a heated 6.35 mm (1/4 in.) copper tube from a fitting mounted in Port E with its tip at approximately the same location as the sampling line for the NDIR analyses. The sample was pulled through the sampling line and flow cell by a small pump located downstream from the flow cell, and then returned to the collection chamber through Port A. There were no traps or filters in this sampling line. The pump flow was measured at 10 L/min maximum, but was at times lower due to fouling of the sampling lines with smoke deposits.

In general, lower limits of FTIR detection for the gases were desired. For example, the 30-minute LC_{50} value (150 µL/L in the N-gas model¹⁴) for HCN is only a few times the minimum detection limit in this instrument. Improved signal to noise ratios were achieved by sampling through the side of the center channel of the chimney, approximately 7 cm below the top. At this location, the effluent volume fractions were significantly higher than they were in the collection chamber since the flow had not yet been diluted into 200 L of air. Presumably the effluent undergoes no further chemistry once past the chimney sampling location and into the cool, well-mixed gas in the collection chamber. Thus, ideally, the ratio of the volume fraction of a trace gas in the chimney to the volume fraction of a more easily quantifiable gas, such as CO₂, in the chimney should be the same as the ratio of the volume fractions of the gases in the collection chamber. However, because the test apparatus is designed to recirculate gas from the collection chamber to the combustion chamber, an unknown fraction of the gas passing the chimney sampling port is from the collection chamber rather than the sample, having already been “counted” on a previous trip up the chimney. So instead, we used the *average* volume fractions in the chimney over the course of the sample burn, and then related this to the *final* volume fraction in the collection chamber. The signal to noise ratio was also improved by averaging up to several hundred spectra prior to quantification.

In a typical run, gas was sampled (for FTIR analysis) from the chimney from the start of the test until flaming ceased. The sampling was then switched to the Port E sampling location by rotating a T-valve fitting that was connected, via more heated copper tube, to the flow cell.

It was not possible to observe the flame height in the chimney, and for a number of the tests, the flame extended out of the chimney and a few centimeters into the collection chamber. This meant that the combustion products could be undergoing reaction downstream of the sampling port, and that the volume fractions extracted from the chimney were not necessarily the final values. The magnitude of the error introduced by this phenomenon was estimated as follows.

- In all the tests, CO₂ was the dominant carbon-containing gas; the volume fraction of CO was no more than 10 % of the volume fraction of CO₂. Thus, oxidation of some part of the CO (or other organic species) downstream of the chimney sampling port would not appreciably affect the volume fraction of CO₂.

ⁱⁱⁱ Certain commercial equipment, products, or materials are identified in this document in order to describe a procedure or concept adequately or to trace the history of the procedures and practices used. Such identification is not intended to imply recommendation, endorsement, or implication that the products, materials or equipment are necessarily the best available for the purpose.

- The volume fractions of CO and CO₂ in the collection chamber, which were measured after the specimen flaming had ceased, were indicative of the full flame chemistry. The same is true of the ratio of these two volume fractions.
- Comparing the ratio of the two volume fractions in the chimney to the ratio in the collection chamber provided an indication of the degree of CO oxidation in the extended flame.

A similar process might have been followed for HCN and the other organic combustion products. However, their volume fractions in the collection chamber were too small to be quantified. The procedure for estimating these yields or upper limits of these yields is described in Sections III.F.3 and III.F.4.

HCl is generated soon after the specimen pyrolysis and is not oxidized downstream. Thus, the ratio of the volume fractions of HCl to CO₂ measured in the chimney should be nominally the same as the ratio in the collection chamber.

An example of a spectrum measured by FTIR spectroscopy during one such test is displayed in Figure 6. The series of peaks extending from about 3050 cm⁻¹ to 2600 cm⁻¹ are due to HCl. In this case, it is possible to resolve the individual frequencies corresponding to changes in the population of rotational states as the H-Cl bonds vibrate. This is usually only possible for small gas phase molecules. There are three spectral features due to CO₂ that are evident in this spectrum. The most intense, centered at 2350 cm⁻¹, corresponds to asymmetric stretching of the two C=O bonds. The symmetric stretch is not observed because there is no change in dipole moment when both O atoms move in phase. The second feature, seen as two distinct peaks centered at about 3650 cm⁻¹, is an overtone band that derives from the simultaneous excitation of these bond-stretching modes. The third peak at about 650 cm⁻¹ is due to the out of plane bending of the molecule. There are bands due to the C≡O stretching vibrations in carbon monoxide, centered at about 2150 cm⁻¹. The remaining peaks in this spectrum are due to H₂O.

Using these spectra, gas concentrations were quantified using the Autoquant software. This is a software package for performing real time and off-line quantitative analyses of target compounds, and is based on the Classical Least Squares (CLS) algorithm as described by Haaland *et al.*²⁵ In this method, the measured spectra are fit to linear combinations of reference spectra corresponding to the target compounds.

Calibration spectra were obtained from a quantitative spectral library assembled by Midac²⁶ and from a collection of spectra provided the Federal Aviation Administration who performed bench-scale fire tests on similar materials.²⁷ In this analysis, the least squares fits were restricted to characteristic frequency regions or windows for each compound that were selected in such a way as to maximize the discrimination of the compounds of interest from other components present in fire gases. All reference spectra were recorded at 170 °C and ambient pressure.

The identities of the target compounds (as well as other compounds that absorb at the same frequencies and must, therefore, be included in the analyses), their corresponding concentrations (expressed in units of μL/L for a mixture of the calibration gas and N₂ in a 1 meter cell), and the characteristic spectral windows used in the quantitative analyses are listed in Table 5.

Also listed in this Table are minimum detection limits (MDLs) for each of the target compounds. These values, which represent the lowest concentrations that can be measured with the instrumentation employed in these tests, were estimated as follows. The calibration spectra were added to test spectra (which, when possible, were selected in such a way that only the compound of interest was not present) with varying coefficients until the characteristic peaks of the target compounds were just discernible above the baseline noise. The value of signal averaging over *ca.* 100 spectra was included. The MDL values reported in Table 5 were obtained by multiplying these coefficients by the known concentrations of the target compound in the calibration mixtures.

Water, methane and acetylene are included in the quantitative analyses because they have spectral features that interfere with the target compounds. The nitrogen oxides absorb in the middle of the water band that extends from about 1200 cm^{-1} to 2050 cm^{-1} . Consequently, the limits of detection for these two compounds are higher than for any of the other target compounds. Thus, it is not surprising that their presence was not detected in any of the tests.

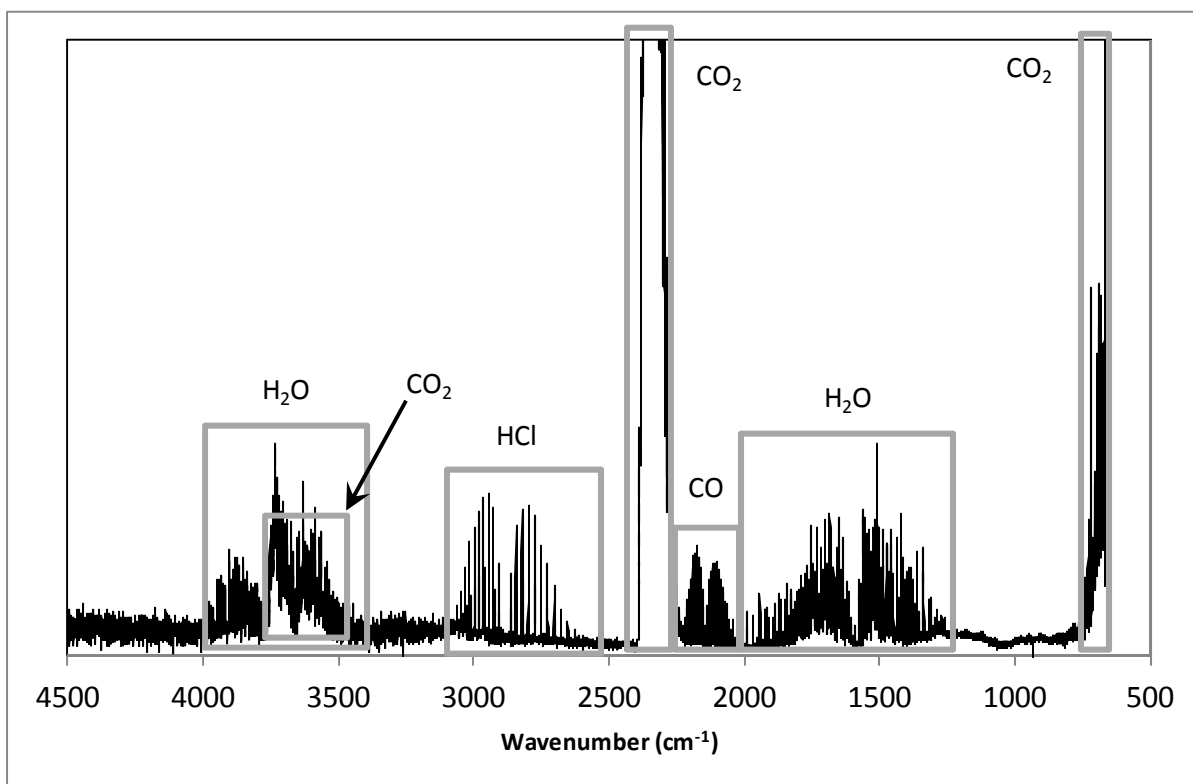


Figure 6. FTIR Spectrum of the Products of Burning Electrical Cable.

Table 5. Species and Frequency Windows for FTIR Analysis.

Compound	Reference Volume Fraction ($\mu\text{L/L}$)	Frequency Window (cm^{-1})	Minimum Detection Limit ($\mu\text{L/L}$)
CH_4	483	2800 to 3215	20
$\text{C}_3\text{H}_4\text{O}$	2250	850 to 1200	20
CH_2O	11300	2725 to 3000	40
CO_2	47,850	660 to 725, 2230 to 2300	800 ^a
CO	2410	2050 to 2225	20
H_2O	100,000	1225 to 2050, 3400 to 4000	130 ^a
HCl	9870	2600 to 3100	20
HCN	507	710 to 722, 3200 to 3310	35
NO	512	1870 to 1950	70
NO_2	70	1550 to 1620	40

^a Present in the background.

Delay times for gas flows from the sampling locations within the test structure to the gas analyzers were small compared to the duration of the specimen burning. The burn durations were at least 2 min for the bookcase specimens, at least 2 min for the cable specimens, and at least 1 min for the sofa specimens. Combining the gas sample pumping rate and the volumes of the sampling lines, the delay time to the oxygen analyzer was about 5 s, about 1 s to the CO and CO_2 analyzers, and 0.1 s to the FTIR analyzer. Since the yield calculations involved averaged volume fractions over the duration of the burning, delay time effects were neglected.

B. Operating Procedures

1. "Standard" Testing

The intent was to test specimens of each of the three finished products in the manner prescribed in the two Standards, although without the use of test animals. The steps in the procedure are:

- Calibrate the heat flux to the specimen surface and calibrate the gas analyzers (each performed daily).
- Weigh the specimen holder without and with the test specimen.
- Open the shutter.
- Insert the test specimen on the specimen holder and cap the combustion cell.
- Turn on the gas sampling system and establish background data for the combustion product concentrations and baseline data for the initial specimen mass.
- Turn on the quartz heaters and turn on the spark igniter.

- Record the time of ignition and turn off the spark igniter.
- Record the time of flameout.
- Fifteen minutes after turning on the igniter and heaters, turn off the power to the heaters.
- Collect concentration data for a total of 30 min.
- Dispose of any residue of the test specimen and prepare for the next test.

As prescribed in the two Standards, the specimen mass is to be such that the estimated value of the Fractional Effective Dose (FED) for a 30 min exposure of rats to the effluent is near unity.^{14,15} Preliminary tests were performed to approximate this specimen mass.

During preliminary tests, it was observed that the specimens of the bookcase material continued to smolder after the flames disappeared, and specimens of the power cable continued to pyrolyze. Since the purpose of the small-scale tests was to obtain data for pre- and post-flashover flaming combustion, inclusion of the smoldering/pyrolysis effluent in the collection chamber environment would be misleading. (In the room tests, there was no sustained external heating of the burning finished goods.) Thus, upon observation of flameout, the shutter was immediately closed and the power to the heaters turned off. At the same time, to minimize the risk of a flame puff upon opening the combustion chamber, the chamber was flushed with nitrogen to quench all reaction.

2. Test Specimens

Consistent with the standard procedure, we maintained a specimen configuration that approximated the full combustible item. The initial sofa specimens were a single piece of foam, 7.5 cm by 7.5 cm by 1 cm thick, covered with a single piece of the polyester/cotton cover fabric, 7.5 cm x 7.5 cm, on the upper (exposed) surface. The initial bookcase specimens were single, 7.5 cm x 10 cm pieces of the particle board, with the vinyl surface facing the radiant heaters. The initial cable specimens were three 7.5 cm lengths of cable cut from the spool. Sample sizes were chosen to produce a Fractional Effective Dose (FED) near 1, as determined by the N-gas model for lethality to rats.^{14,15}

$$\begin{aligned} FED &= \frac{m \cdot \varphi_{CO}}{\varphi_{CO_2} - b} + \frac{21\% - \varphi_{O_2}}{21\% - LC_{50} O_2} + \frac{\varphi_{HCN}}{LC_{50} HCN} + \frac{\varphi_{HCl}}{LC_{50} HCl} + \frac{\varphi_{HBr}}{LC_{50} HBr} \\ &= \frac{m \cdot \varphi_{CO}}{\varphi_{CO_2} - b} + \frac{21\% - \varphi_{O_2}}{21\% - 5.4\%} + \frac{\varphi_{HCN}}{150 \mu\text{L/L}} + \frac{\varphi_{HCl}}{3700 \mu\text{L/L}} + \frac{\varphi_{HBr}}{3000 \mu\text{L/L}} \end{aligned}$$

φ_x is the volume percent of CO₂ or O₂ (100 · L/L) and the volume fraction in μL/L for the other gases above. m and b are empirically determined constants such that if $\varphi_{CO_2} < 5\%$ then $m = -18$ and $b = 122,000$; whereas if $\varphi_{CO_2} > 5\%$ then $m = 23$ and $b = -38,600$. Little effort was made to fine-tune the FED, since animals were not being exposed to the effluent.

3. Test Procedure Variation

One of the purposes of this program was to obtain effluent composition data in tests with variants on the standard operating procedure. This would enable estimation of the sensitivity of the gas yields to the manner in which the test specimen was derived from the complete combustible object and examination of the potential for an improved relationship with the yield data from the room-scale tests. For this apparatus, two such variations were examined:

- Variation of the combustion environment to more closely approach the post-flashover conditions that occurred in the room-scale tests. This entailed changing the initial oxygen volume fraction. During pre-flashover burning, the air entrained by a fire has an oxygen volume fraction of nominally 0.21. This fraction is lower for post-flashover fires. Preliminary experiments indicated that flaming combustion of specimens from all three finished products could be initiated for an initial oxygen volume fraction in the collection chamber as low as 0.17. This atmosphere was created by flowing nitrogen into the collection chamber prior to the start of a test until the oxygen analyzer indicated a steady oxygen volume fraction of 0.17.
- Test specimen conformation. To determine the importance of specimen inhomogeneity (e.g., due to layering of the component materials), the test specimens from the sofas and bookcases were cut into pieces with dimensions on the order of 1 cm and randomly arranged in the sample holder. The cable specimens were cut into lengths less than 1 cm and the insulating materials separated. For these diced specimens, (a) materials from the interior of the finished product were directly exposed to the radiant flux and ambient atmosphere and (b) the surface area available for combustion or pyrolysis was increased. In each case the quantity of material was the same mass as that used in the intact specimen (generally approximately 90 g, 6 g, and 30 g for the particleboard, foam, and cable, respectively.) Figure 7 presents photographs of the intact and diced test specimens.



Figure 7. Photographs of Test Specimens.

C. Data Collection

The signals from the load cell and the fixed gas analyzer were collected using a personal computer with National Instruments data acquisition hardware and software. Values were recorded at 1 s intervals. The FTIR spectra were recorded using the FTIR computer system. Spectra were taken every 1 s to 6 s.

During each test, four times were recorded manually. These were the start of test, first observed flaming, cessation of visible flaming, and conclusion of the test. Additional notes were recorded, such as failure of an instrument, clogging of a sampling line, and flames extending above the top of the chimney.

III. CALCULATION METHODS

A. Nomenclature

The following nomenclature is used in this section:

F	carbon mass fraction in the fuel (dimensionless)
Δm	mass loss of the test specimen (g)
M	molecular weight (kg kmol^{-1})
p	pressure (Pa)
T	temperature (K)
y	species yield (dimensionless)
α	combustion expansion factor (dimensionless)
ε	combustion efficiency (dimensionless)
φ	volume fraction of gas g (dimensionless) = p_g / p_T
Φ	global equivalence ratio (dimensionless)
ρ	gas density (kg m^{-3})
V	volume of the collection chamber (L)

Superscripts

A	refers to concentrations in the analyzer
C	refers to concentrations near the top of the chimney
EC	refers to concentrations in the collection chamber

Subscripts

amb	ambient air
dry	dry air
f	fire
g	a gas, g
x	refers to a specific gas of interest, e.g., CO, CO ₂
not	refers to the notional yield of a combustion product
t	total

B. Mass Loss Rate

The specimen mass loss during a test was determined from the initial and final readings from the load cell. The uncertainty in the mass loss was derived from the uncertainties in these two measurements. The noise in these measurements was reduced by using the average of 10 points. Care was taken to allow the specimen holder to cool before the final measurements to cool so that thermal buoyancy would not affect the measured value of the specimen residue. No consideration was given to whether the chemical composition of the residue (if any) was different from the composition of the specimen at the beginning of the test. Mass loss percentages were calculated from the load cell data using the previously identified initial and final readings, and the instantaneous reading to calculate mass lost up to that point.

C. Notional Gas Yields

The notional, or maximum possible, gas yields (Table 6) were calculated as follows:

- CO₂: Assume all the carbon in the test specimen is converted to CO₂. Multiply the mass fraction of C in the test specimen (Table 2 or Section II.C) by the ratio of the molecular mass of CO₂ to the atomic mass of carbon.
- CO: Assume all the carbon in the test specimen is converted to CO. Multiply the mass fraction of C by the ratio of the molecular mass of CO to the atomic mass of carbon.
- HCN: Assume all the nitrogen in the test specimen is converted to HCN. Multiply the mass fraction of N by the ratio of the molecular mass of HCN to the atomic mass of nitrogen.
- HCl: Assume all the chlorine in the test specimen is converted to HCl. Multiply the mass fraction of Cl by the ratio of the molecular mass of HCl to the atomic mass of chlorine.

The notional yields from the bookcase and cable specimens were assumed to be the same as the yields from the intact combustibles.¹⁶ The sofa specimen had a mass ratio of fabric to foam that differed modestly from the intact sofas.

Table 6. Calculated Notional Yields of Toxic Products from the Test Specimens.

Gas	Notional Yields		
	Bookcase	Cable	Sofa
			1 layer foam
CO ₂	1.72 ± 1 %	2.11 ± 1 %	1.95 ± 4 %
CO	1.09 ± 1 %	1.33 ± 1 %	1.24 ± 4 %
HCN	0.057 ± 13 %	0.040 ± 6 %	0.193 ± 4 %
HCl	0.0026 ± 4 %	0.332 ± 1 %	0.0069 ± 19 %

The uncertainty in the notional yield values is determined by the uncertainty in the prevalence of the central element (in the bullets just above) in the combustible. These uncertainties were estimated in Section I.C. For the cuttings from the sofas, the uncertainty in the notional yields

was increased by the small variability (estimated at 3 percent) in the relative masses of the fabric and padding materials in the test specimens.

D. Calculated Gas Yields

1. CO and CO₂

Yields of CO and CO₂ were calculated using the volume of the collection chamber, the gas concentrations in the chamber (accounting for the background concentrations in room air), the consumed mass of the fuel, and the ideal gas law.

$$p_g V = m_g R T/M_g$$

$$y_g = [\rho_g p_t V M_g] / [R T \Delta m_{fuel}]$$

where R is the universal gas constant, 8.31×10^3 L-Pa/mol-K. The pressure, temperature, gas volume fractions, and mass lost from the test specimen were all measured in the laboratory.

We soon discovered that the CO₂ absorption band used by the FTIR spectrometer software was saturated, so that the FTIR peak intensity was not proportional to the volume fraction. Accordingly, we calculated the area under the CO₂ absorption band for a number of volume fractions and plotted the results against the FTIR spectrometer software values for known CO₂/air mixtures. This is shown in Figure 8. This enabled determining the relationships of volume fractions of other gases measured in the chimney to their volume fractions in the collection chamber. The concentrations of the other gases were sufficiently low that their absorption bands were not saturated.

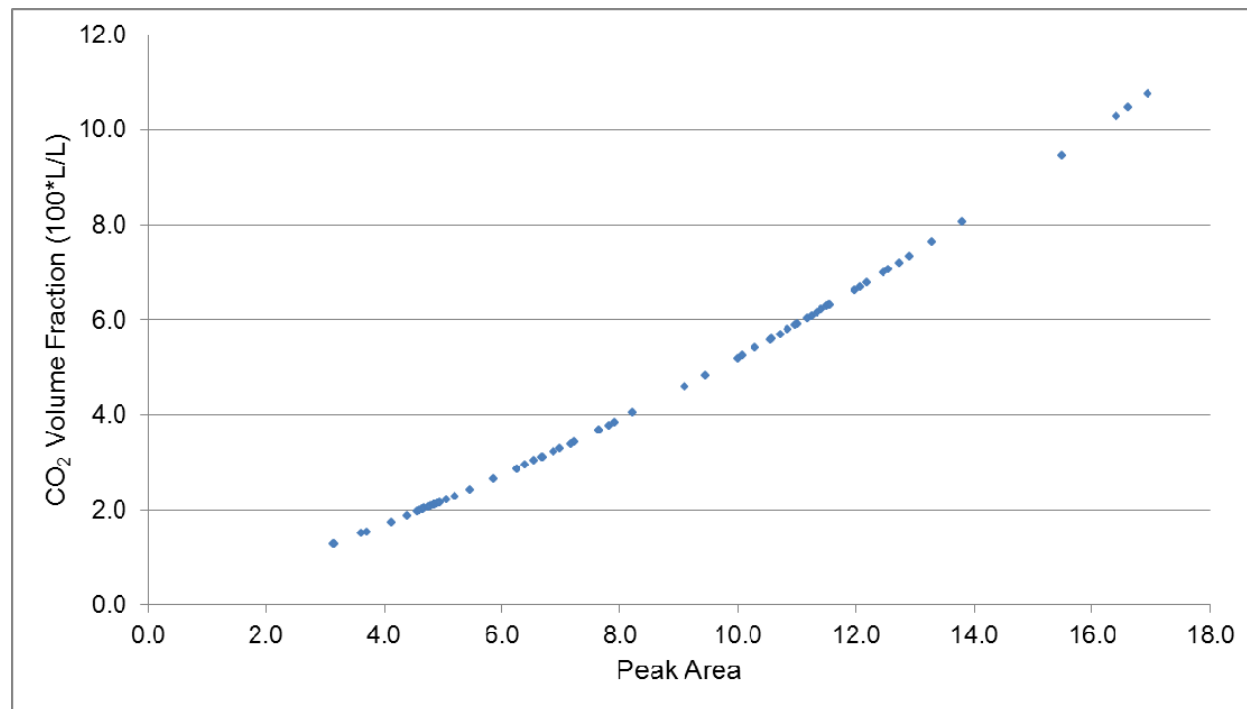


Figure 8. CO₂ Volume Fraction vs. Peak Area.

A plot of the values of $[\varphi_{CO}/\varphi_{CO_2}]_{chamber}$ vs. $[\varphi_{CO}/\varphi_{CO_2}]_{chimney}$ did not show the expected linear relationship with an intercept at the origin (Figure 9). Figure 9 suggests that when the combustion at the sampling point is relatively efficient (between < 1 percent CO by volume and 4 percent CO by volume), partial oxidation of pyrolyzate leads to a relatively constant CO concentration emanating from the reaction volume. As the combustion becomes less complete, pyrolyzate oxidation and CO burnout in the plume proceed at comparable rates. At any rate, the CO volume fractions in the chamber were always large enough that the measurements there could be used to calculate the CO yields.

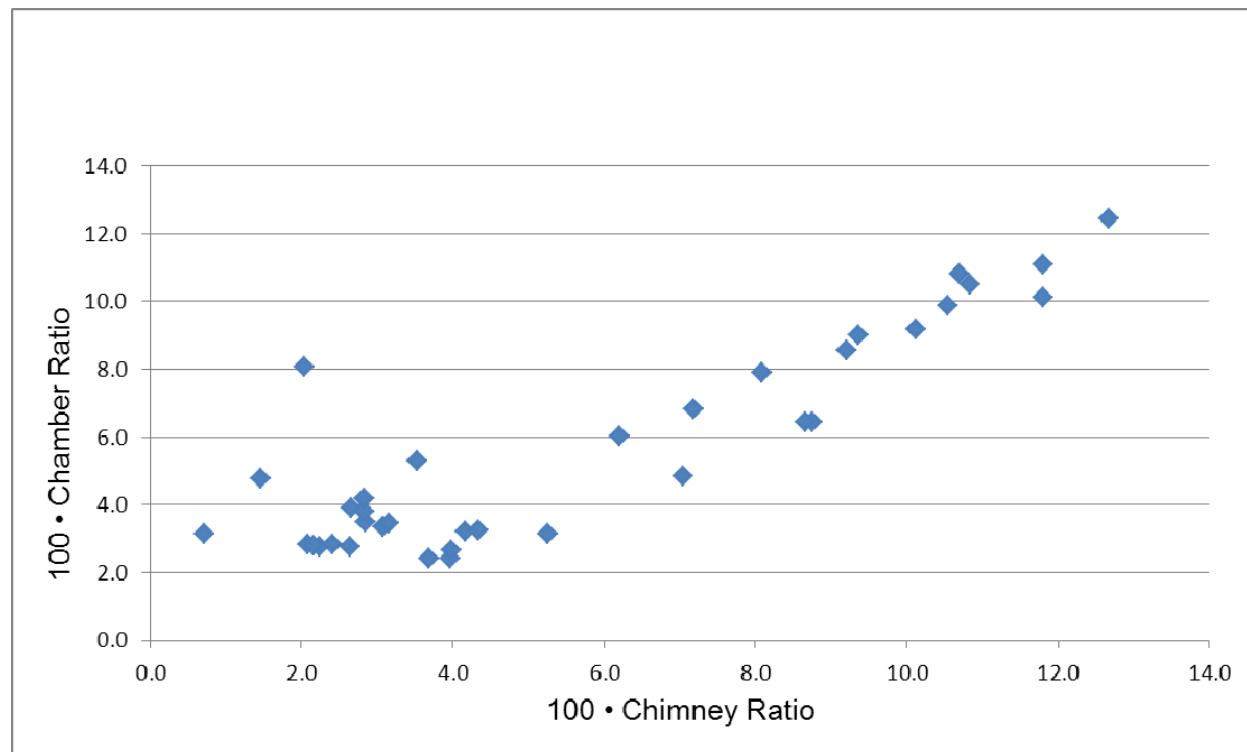


Figure 9. $[\varphi_{CO}/\varphi_{CO_2}]_{chamber}$ vs. $[\varphi_{CO}/\varphi_{CO_2}]_{chimney}$.

Another consideration for the yield calculations was the value of the chamber volume. During the course of a test, the expansion bag inflated both due to the temperature rise in the collection chamber and to the additional gaseous combustion products from the burning test specimen.

- The initial temperature in the chamber was typically 296 K and the typical temperature rises were to approximately 330 K or lower. Thus, the peak volume expansion from this source was about 10 %. After the burning had ceased, the gas in the chamber cooled due to contact with the chamber walls, and the temperature returned essentially to room temperature. Thus, by using the *final* volume fractions of the two gases in calculating the gas yields, it was consistent to use the chamber volume with the bag deflated.
- The specimen combustion ceased when the fuel was consumed or when the oxygen volume fraction in the chamber neared 0.14. For this amount of oxygen consumption,

calculations for complete combustion of either a hydrocarbon fuel (i.e., containing no oxygen) or a wood-like fuel indicate that the generated combustion gases would expand the volume by about 3 % or 7 %, respectively. This contribution to the bag expansion would not change as the chamber gases cooled. However, some of the combustion products (e.g., much of the water vapor) would condense as the temperature dropped or would be adsorbed on the chamber surfaces. Thus, at the end of the test, the increase in the gas volume would be of the order of 5 % or less and was neglected.

For each experiment, the uncertainty in the yield values for these two gases resulted from:

- The uncertainty in the volume fraction measurement in the chimney. This was typically less than 5 percent.
- The uncertainty in the specimen mass loss. This was typically less than 1 percent.
- The uncertainty in the collection chamber volume. This was on the order of 1 percent.

We therefore assigned a numerical uncertainty of \pm 5 percent to the yields of CO and CO₂.

There was also a contribution to the repeatability of the test results from variation in the combustion of each test specimen. As will be seen below, this was generally larger than the above uncertainties.

2. HCl

The only calculable HCl yields were from the cable specimens. Above the chimney sampling point, HCl should not have been generated or consumed by any flames extending through the chimney. The yields were calculated by multiplying the yield of CO₂ by the ratio of the volume fraction of HCl in the chimney to the volume fraction of CO₂ in the chimney and the ratio of molecular weights of the two gases. The estimated uncertainty in the HCl volume fractions was \pm 10 percent, and the estimated uncertainty in the HCl yields was \pm 15 percent.

3. HCN

There were some calculable HCN yields from the sofa and cable specimens. The HCN volume fractions in the chamber were close to the limit of detection; thus, it was preferred to calculate HCN yields using the volume fractions in the chimney. However, as with CO, there is the potential for HCN to be oxidized to nitrogen oxides downstream of the chimney sampling location. To the extent that this occurs, the HCN volume fraction emerging from the flame would be overestimated.

An estimate of the degree of HCN oxidation was obtained as follows. For those tests in which there were measurable volume fractions of HCN in both the chamber and the chimney, the ratio of the volume fractions of CO₂ in the two locations was 2.9 ± 0.2 . The ratio for the HCN volume fractions was 5.5 ± 1.8 . The greater variability in the latter ratio was likely due to the closeness of some of the chamber volume fractions to the limit of detection and to differences in the flame extension beyond the sampling point. Of more importance is the fact that the HCN ratio is approximately double the CO₂ ratio, indicating that typically about half of the HCN had been oxidized before entering the chamber.

As a result, the yields of HCN were estimated by multiplying the yield of CO₂ by the ratio of the volume fraction of HCN in the chimney to the volume fraction of CO₂ in the chimney, then by the ratio of molecular weights. The results were then divided by two as an estimate of the oxidized fraction:

$$y_{\text{HCN}} = \frac{1}{2} y_{\text{CO}_2} (\varphi_{\text{HCN, chimney}} / \varphi_{\text{CO}_2, \text{chimney}}) (M_{\text{HCN}} / M_{\text{CO}_2})$$

The estimated uncertainty in the larger values of the HCN volume fraction was ± 25 percent, and the estimated uncertainty in the HCN yields was ± 30 percent. The uncertainty increased as values of φ_{HCN} approached the limit of detection.

4. Other Gases

The volume fractions of the other toxic gases in both the chimney and the collection chamber were always below the detection limit. Thus, the upper limits of the yields of these gases were estimated using their limits of detection.

IV. RESULTS

A. Tests Performed

The following is the test numbering key, with format F-Y-m-[O₂]-N, where

- F: Fuel [S = sofas; B = bookcases; P = power cable]
- Y: 1 = intact specimen; 2 = diced specimen
- m: Approximate initial specimen mass (g). For the sofa specimens, this is followed by the number of layers of fabric and of foam.
- [O₂] Approximate initial oxygen volume percent in the collection chamber
- N: Replicate test number for that set of combustible and conditions

Some of the replicate runs are not included if an instrument failed or if one of the sampling lines became clogged.

Table 7 through Table 12 present the test data and the calculated yields for the bookcase, sofa, and cable specimens, respectively. In these tables, Δt is the observed duration of flaming combustion and Δm is the measured mass lost during the flaming combustion. The horizontal colored bands highlight groups of replicate tests. A yield number in red indicates a higher uncertainty due to the volume fraction being near the limit of detection.

All yields were calculated from NDIR volume fractions (CO, CO₂) or referenced to the NDIR values for CO₂ (HCN, HCl). The mean ratio of NDIR volume fraction values to FTIR volume fraction values for CO₂ was 0.86 ± 0.24 ; the ratio for CO was a nearly identical 0.85 ± 0.24 . Figure 10 shows there was not a strong dependence of this ratio on the type of specimen or the completeness of combustion.

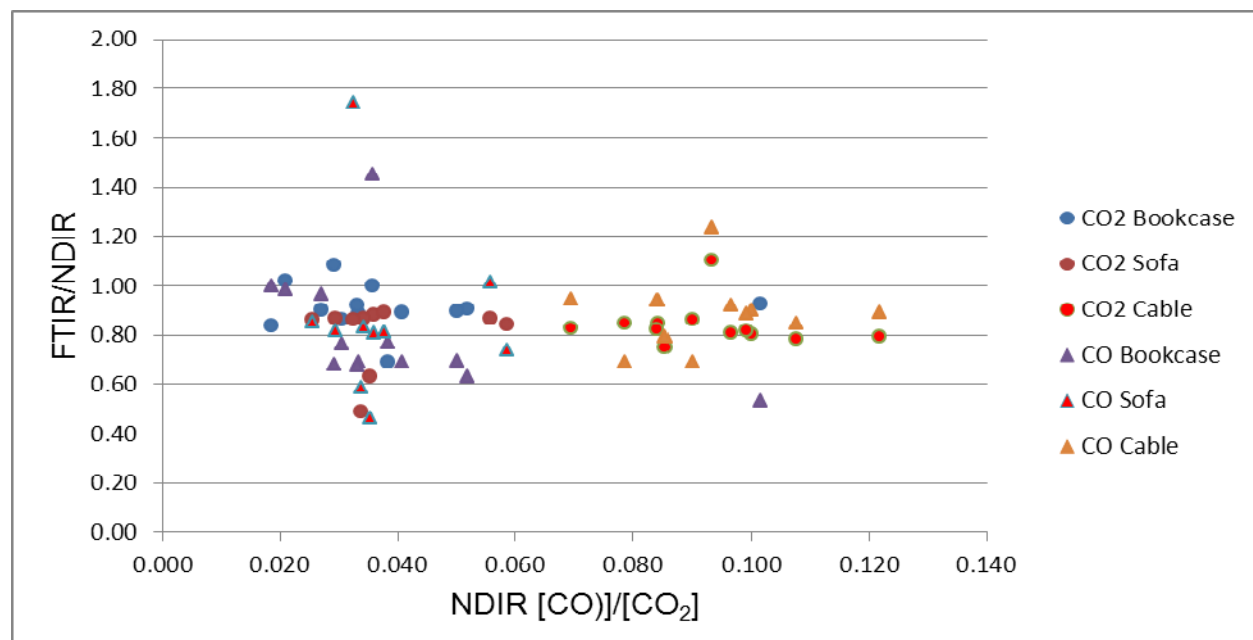


Figure 10. Ratios of CO₂ and CO volume fractions measured using NDIR and FTIR spectroscopy vs. the NDIR CO/CO₂ volume fraction ratio.

Table 7. Data from Bookcase Material Tests.

Code	Size	Specimen Mass (g)	Δm (g)	Δt (s) Flaming	NDIR Chamber		Final M_{O_2} (L/L)	FTIR (Chamber)			FTIR (Chimney)			
					M_{CO_2} (L/L)	M_{CO} (:L/L)		M_{CO_2} (L/L)	M_{CO} (:L/L)	M_{HCN} (:L/L)	M_{CO_2} (L/L)	M_{CO} (:L/L)	M_{HCN} (:L/L)	
B-1-90-21-2	slab 76 x95x20	90.9	29.6	313	0.0706	2530	0.135	0.0706	3670	110	0.0805	1360	0	110
B-1-90-21-3	slab 76 x95x20	88.1	26.9	195	0.0618	3200	0.145	0.0560	2020	100	0.1046	910	0	30
B-1-90-21-4	slab 76 x95x20	87.8	25.6	270	0.0608	1270	0.145	0.0621	1250	0	0.0630	1200	0	0
B-1-90-21-5	slab 76 x95x20	89.4	25.3	235	0.0628	1160	0.143	0.0526	1160	30	0.0678	980	0	10
B-1-90-21-6	slab 76 x95x20	89.6	29.5	293	0.0700	2680	0.136	0.0483	2060	20	0.0699	1680	0	30
B-2-90-21-1	diced cubes	90.3	24.9	150	0.0629	2100	0.143	0.0558	1450	50	0.1027	1700	0	110
B-2-90-21-4	diced cubes	88.7	23.7	140	0.0567	1660	0.148	0.0615	1130	20	0.0764	380	0	70
B-2-90-21-5	diced cubes	90.0	25.6	161	0.0632	1710	0.142	0.0570	1650	40	0.0946	1630	0	40
B-1-90-17-1	slab 76 x95x20	89.8	14.4	110	0.0332	1010	0.137	0.0286	770	0	0.0628	1020	0	10
B-1-90-17-2	slab 76 x95x20	92.1	18.2	148	0.0410	1360	0.131	0.0378	920	0	0.0662	970	0	0
B-2-90-17-1	diced cubes	90.4	16.6	98	0.0348	1420	0.136	0.0311	980	0	0.0734	1500	0	0
B-2-90-17-2	diced cubes	90.4	18.9	148	0.0383	1920	0.133	0.0343	1330	40	0.0720	1420	0	90

Table 8. Gas Yields from Bookcase Material Tests.

Code	Size	Specimen Mass (g)	Δm (g)	y_{CO_2} (g/g)	y_{CO} (g/g)	y_{HCN} (g/g)	y_{HCl} (g/g)	y_{NO} (g/g)	y_{NO_2} (g/g)	$Y_{acrolein}$ (g/g)	y_{form} (g/g)
B-1-90-21-2	slab 76 x95x20	90.9	29.6	0.88	0.0200	< 0.00012	0.00097	< 0.0005	< 0.0005	< 0.0003	< 0.0003
B-1-90-21-3	slab 76 x95x20	88.1	26.7	0.85	0.0279	< 0.00009	0.00020	< 0.0004	< 0.0003	< 0.0002	< 0.0002
B-1-90-21-4	slab 76 x95x20	87.8	25.5	0.88	0.0115	< 0.00015	< 0.00000	< 0.0007	< 0.0006	< 0.0004	< 0.0004
B-1-90-21-5	slab 76 x95x20	89.4	26.0	0.92	0.0106	< 0.00015	< 0.00011	< 0.0006	< 0.0006	< 0.0004	< 0.0004
B-1-90-21-6	slab 76 x95x20	89.6	30.5	0.88	0.0213	< 0.00013	0.00030	< 0.0006	< 0.0005	< 0.0004	< 0.0003
B-2-90-21-1	diced pieces	90.3	35.9	0.93	0.0197	< 0.00010	0.00081	< 0.0004	< 0.0004	< 0.0003	< 0.0002
B-2-90-21-4	diced pieces	88.7	24.8	0.88	0.0163	< 0.00012	0.00065	< 0.0005	< 0.0005	< 0.0003	< 0.0003
B-2-90-21-5	diced pieces	90.0	27.1	0.91	0.0156	< 0.00010	0.00031	< 0.0005	< 0.0004	< 0.0003	< 0.0003
B-1-90-17-1	slab 76 x95x20	89.8	15.4	0.85	0.0162	< 0.00015	< 0.00022	< 0.0006	< 0.0006	< 0.0004	< 0.0004
B-1-90-17-2	slab 76 x95x20	92.1	18.7	0.83	0.0174	< 0.00013	< 0.00020	< 0.0006	< 0.0005	< 0.0004	< 0.0003
B-2-90-17-1	diced pieces	90.4	17.8	0.77	0.0199	< 0.00011	< 0.00017	< 0.0005	< 0.0004	< 0.0003	< 0.0003
B-2-90-17-2	diced pieces	90.4	19.6	0.75	0.0237	< 0.00011	0.00075	< 0.0005	< 0.0004	< 0.0003	< 0.0003

Table 9. Data from Sofa Material Tests.

Code	Size	Specimen Mass (g)	Δm (g)	Δt (s) Flaming	NDIR Chamber		Final M_{O_2} (L/L)	FTIR (Chamber)				FTIR (Chimney)			
					M_{CO_2} (L/L)	M_{CO} (:L/L)		M_{CO_2} (L/L)	M_{CO} (:L/L)	M_{HCl} (:L/L)	M_{HCN} (:L/L)	M_{CO_2} (L/L)	M_{CO} (:L/L)	M_{HCN} (:L/L)	M_{HCl} (:L/L)
5-1-6,1&1,21-1	76x64x25	6.1	5.4	123	0.0264	890	0.176	0.0129	520	0	30	0.0243	760	20	0
S-1-6,1&1-21-2	76x64x25	6.1	5.4	79	0.0239	610	0.180	0.0206	520	0	90	0.0580	1590	380	40
S-1-6,1&1-21-3	76x64x25	6.2	5.4	73	0.0238	470	0.180	0.0151	490	0	0	corrupt	corrupt	corrupt	corrupt
S-2-6,1&1-21-1	diced pieces	6.3	5.3	67	0.0244	720	0.180	0.0212	590	20	60	0.0541	1620	310	40
S-2-6,1&1-21-2	diced pieces	6.3	5.5	64	0.0245	880	0.179	0.0216	710	30	120	0.0592	2250	450	50
S-1-6,1&1-17-1	76x64x25	6.3	5.5	77	0.0244	860	0.144	0.0154	400	0	30	0.0404	1300	60	0
S-1-6,1&1-17-2	76x64x25	6.2	5.6	70	0.0238	900	0.143	0.0212	730	0	10	0.0520	1650	70	0
S-1-6,1&1-17-3	76x64x25	6.5	5.8	90	0.0250	810	0.142	0.0215	1410	10	50	0.0608	3810	190	0
S-2-6,1&1-17-1	diced pieces	6.3	5.4	59	0.0246	840	0.143	0.0213	700	0	40	0.0589	1820	330	0
S-2-6,1&1-17-2	diced pieces	6.3	5.2	55	0.0235	1380	0.147	0.0198	1020	0	90	0.0670	3250	730	0
S-2-6,1&1-17-3	diced pieces	6.3	5.8	60	0.0249	1390	0.143	0.0216	1410	10	50	0.0603	3790	265	0

Table 10. Gas Yields from Sofa Material Tests.

Page	Code	Size	Specimen Mass (g)	Δm (g)	y_{CO_2} (g/g)	y_{CO} (g/g)	y_{HCN} (g/g)	y_{HCl} (g/g)	y_{NO} (g/g)	y_{NO_2} (g/g)	$Y_{acrolein}$ (g/g)	y_{form} (g/g)
109	5-1-6,1&1,21-1	76x64x25	6.1	5.4	1.80	0.038	< 0.00079	< 0.00119	< 0.0035	< 0.0031	< 0.0021	< 0.0020
110	S-1-6,1&1-21-2	76x64x25	6.1	5.4	1.62	0.026	0.00327	0.00090	< 0.0013	< 0.0014	< 0.0006	< 0.0014
136	S-1-6,1&1-21-3	76x64x25	6.2	5.4	1.62	0.020						
111	S-2-6,1&1-21-1	diced pieces	6.3	5.3	1.69	0.031	0.00297	0.00101	< 0.0015	< 0.0016	< 0.0006	< 0.0016
112	S-2-6,1&1-21-2	diced pieces	6.3	5.5	1.63	0.037	0.00381	0.00111	< 0.0013	< 0.0014	< 0.0006	< 0.0014
120	S-1-6,1&1-17-1	76x64x25	6.3	5.5	1.66	0.037	0.00076	< 0.00066	< 0.0020	< 0.0021	< 0.0008	< 0.0021
121	S-1-6,1&1-17-2	76x64x25	6.2	5.6	1.68	0.040	0.00069	< 0.00052	< 0.0015	< 0.0016	< 0.0006	< 0.0016
137	S-1-6,1&1-17-3	76x64x25	6.5	5.8	1.58	0.032	0.00152	< 0.00042	< 0.0012	< 0.0013	< 0.0005	< 0.0013
122	S-2-6,1&1-17-1	diced pieces	6.3	5.4	1.64	0.035	0.00282	< 0.00045	< 0.0013	< 0.0014	< 0.0006	< 0.0014
123	S-2-6,1&1-17-2	diced pieces	6.3	5.2	1.54	0.057	0.00515	< 0.00037	< 0.0011	< 0.0011	< 0.0005	< 0.0011
138	S-2-6,1&1-17-3	diced pieces	6.3	5.8	1.58	0.056	0.00213	< 0.00042	< 0.0012	< 0.0013	< 0.0005	< 0.0013

Table 11. Data from Cable Material Tests.

Code	Size	Specimen Mass (g)	Δm (g)	NDIR Chamber			Final M_{O_2} (L/L)	FTIR (Chamber)			FTIR (Chimney)			
				Δt (s) Flaming	M_{CO_2} (L/L)	M_{CO} (:L/L)		M_{CO_2} (L/L)	M_{CO} (:L/L)	M_{HCl} (:L/L)	M_{CO_2} (L/L)	M_{CO} (:L/L)	M_{HCN} (:L/L)	M_{HCl} (:L/L)
C-1-30-21-3	3 x 127 mm	29.6	8.2	162	0.0242	2180	0.176	0.0209	1500	805	0.0322	1560	160	5120
C-1-30-21-4	3 x 127 mm	29.6	7.5	166	0.0262	2060	0.174	0.0222	1420	2479	0.0368	1850	120	6640
C-1-30-21-5	3 x 127 mm	29.6	8.2	186	0.0250	2110	0.174	0.0212	1990	23	0.0303	2650	40	7400
C-1-30-21-6	3 x 127 mm	29.7	7.7	147	0.0245	2060	0.174	0.0201	1939	3420	0.0368	3240	40	10060
C-1-30-21-7	3 x 127 mm	30.0	7.5	115	0.0232	2240	0.176	0.0188	2060	4710	0.0460	4320	70	13740
C-2-30-21-2	diced pieces	29.7	8.1	135	0.0269	2300	0.173	0.0202	1820	2500	0.0329	2660	10	7890
C-2-30-21-3	diced pieces	29.3	7.7	157	0.0220	2680	0.179	0.0175	2390	4959	0.0128	1850	10	6140
C-2-30-21-4	diced pieces	29.6	7.6	145	0.0191	1780	0.182	0.0211	2200	4000	0.0339	3190	50	9200
C-1-30-17-1	3 x 127 mm	29.7	8.1	186	0.0259	2790	0.138	0.0203	2360	3990	0.0286	3130	50	9260
C-1-30-17-2	3 x 127 mm	29.7	7.7	180	0.0245	2450	0.140	0.0197	2210	3900	0.0265	2720	30	8600
C-2-30-17-1	diced pieces	29.4	7.3	127	0.0261	2590	0.136	0.0214	2300	4840	0.0312	3110	20	9660
C-2-30-17-2	diced pieces	29.5	6.8	147	0.0259	1800	0.138	0.0214	1700	4530	0.0295	2210	0	8380

Table 12. Gas Yields from Cable Material Tests.

Code	Size	Specimen Mass (g)	Δm (g)	y_{CO_2} (g/g)	y_{CO} (g/g)	y_{HCN} (g/g)	y_{HCl} (g/g)	y_{NO} (g/g)	y_{NO_2} (g/g)	$Y_{acrolein}$ (g/g)	y_{form} (g/g)
C-1-30-21-3	3 x 127 mm	29.6	8.2	1.08	0.057	0.00165	0.14	< 0.0016	< 0.0014	< 0.0009	< 0.0009
C-1-30-21-4	3 x 127 mm	29.6	7.5	1.28	0.059	0.00128	0.19	< 0.0017	< 0.0014	< 0.0010	< 0.0009
C-1-30-21-5	3 x 127 mm	29.6	8.2	1.28	0.059	0.00128	0.19	< 0.0017	< 0.0014	< 0.0010	< 0.0009
C-1-30-21-6	3 x 127 mm	29.7	7.7	1.12	0.055	0.00045	0.22	< 0.0018	< 0.0015	< 0.0010	< 0.0010
C-1-30-21-7	3 x 127 mm	30.0	7.5	1.17	0.057	0.00039	0.26	< 0.0015	< 0.0013	< 0.0009	< 0.0009
C-2-30-21-2	diced pieces	29.7	8.1	1.13	0.064	0.00053	0.27	< 0.0012	< 0.0010	< 0.0007	< 0.0007
C-2-30-21-3	diced pieces	29.3	7.7	1.22	0.061	< 0.00040	0.24	< 0.0018	< 0.0015	< 0.0010	< 0.0010
C-2-30-21-4	diced pieces	29.6	7.6	1.05	0.076	< 0.00088	0.41	< 0.0039	< 0.0034	< 0.0023	< 0.0022
C-1-30-17-1	3 x 127 mm	29.7	8.1	0.92	0.049	0.00042	0.20	< 0.0013	< 0.0011	< 0.0008	< 0.0007
C-1-30-17-2	3 x 127 mm	29.7	7.7	1.17	0.075	0.00063	0.31	< 0.0020	< 0.0017	< 0.0011	< 0.0011
C-2-30-17-1	diced pieces	29.4	7.3	1.17	0.069	< 0.00047	0.31	< 0.0021	< 0.0018	< 0.0012	< 0.0012
C-2-30-17-2	diced pieces	29.5	6.8	1.31	0.077	< 0.00689	0.33	< 0.0020	< 0.0018	< 0.0012	< 0.0011

B. Calculations of Toxic Gas Yields with Uncertainties

Table 13 contains the yields of the combustion products calculated using the data from Table 8, Table 10, and Table 12. The estimated uncertainties reflect the repeatability of the volume fractions in replicate tests, uncertainties in the other terms in the yields calculations, and degree of proximity of the measured values to the background levels.

Table 13. Yields of Combustion Products from Radiant Furnace Tests.

GAS	Initial M_{O_2}	Form	Bookcase	Sofa	Cable
CO ₂	0.21	Intact	0.88 ± 8 %	1.68 ± 10 %	1.16 ± 11 %
	0.21	Diced	0.91 ± 8 %	1.66 ± 7 %	1.13 ± 11 %
	0.17	Intact	0.84 ± 8 %	1.64 ± 8 %	1.05 ± 17 %
	0.17	Diced	0.76 ± 8 %	1.59 ± 8 %	1.24 ± 11 %
CO	0.21	Intact	0.0183 ± 40 %	0.028 ± 32 %	0.058 ± 7 %
	0.21	Diced	0.0172 ± 15 %	0.034 ± 15 %	0.067 ± 15 %
	0.17	Intact	0.0168 ± 8 %	0.036 ± 14 %	0.062 ± 30 %
	0.17	Diced	0.0218 ± 14 %	0.049 ± 26 %	0.073 ± 20 %
HCN	0.21	Intact	< 2 x 10 ⁻⁴	< 3 x 10 ⁻³	9 x 10 ⁻³ ± 65 %
	0.21	Diced	< 1 x 10 ⁻⁴	3.4 x 10 ⁻³ ± 45 %	< 6 x 10 ⁻⁴
	0.17	Intact	< 2 x 10 ⁻⁴	1.0 x 10 ⁻³ ± 70 %	5 x 10 ⁻⁴ ± 50 %
	0.17	Diced	< 1 x 10 ⁻⁴	3.4 x 10 ⁻³ ± 65 %	< 7 x 10 ⁻³
HCl	0.21	Intact	3 x 10 ⁻⁴ ± x3	< 1 x 10 ⁻³	0.20 ± 35 %
	0.21	Diced	6 x 10 ⁻⁴ ± 45 %	1 x 10 ⁻³ ± 25 %	0.31 ± 40 %
	0.17	Intact	< 2 x 10 ⁻⁴	< 7 x 10 ⁻⁴	0.25 ± 40 %
	0.17	Diced	< 8 x 10 ⁻⁴	< 5 x 10 ⁻⁴	0.32 ± 18 %
NO	0.21	Intact	< 7 x 10 ⁻⁴	< 3 x 10 ⁻³	< 2 x 10 ⁻³
	0.21	Diced	< 5 x 10 ⁻⁴	< 2 x 10 ⁻³	< 2 x 10 ⁻³
	0.17	Intact	< 6 x 10 ⁻⁴	< 2 x 10 ⁻³	< 2 x 10 ⁻³
	0.21	Diced	< 5 x 10 ⁻⁴	< 1 x 10 ⁻³	< 2 x 10 ⁻³
NO ₂	0.21	Intact	< 6 x 10 ⁻⁴	< 3 x 10 ⁻³	< 2 x 10 ⁻³
	0.21	Diced	< 5 x 10 ⁻⁴	< 2 x 10 ⁻³	< 3 x 10 ⁻³
	0.17	Intact	< 6 x 10 ⁻⁴	< 3 x 10 ⁻³	< 2 x 10 ⁻³
	0.21	Diced	< 4 x 10 ⁻⁴	< 2 x 10 ⁻³	< 2 x 10 ⁻²
Acrolein	0.21	Intact	< 4 x 10 ⁻⁴	< 2 x 10 ⁻³	< 1 x 10 ⁻³
	0.17	Diced	< 3 x 10 ⁻⁴	< 6 x 10 ⁻⁴	< 1 x 10 ⁻³
	0.17	Intact	< 4 x 10 ⁻⁴	< 8 x 10 ⁻⁴	< 1 x 10 ⁻³
	0.17	Diced	< 3 x 10 ⁻⁴	< 6 x 10 ⁻⁴	< 1 x 10 ⁻³
Formaldehyde	0.21	Intact	< 4 x 10 ⁻⁴	< 2 x 10 ⁻³	< 1 x 10 ⁻³
	0.21	Diced	< 3 x 10 ⁻⁴	< 2 x 10 ⁻³	< 2 x 10 ⁻³
	0.17	Intact	< 4 x 10 ⁻⁴	< 2 x 10 ⁻³	< 1 x 10 ⁻³
	0.17	Diced	< 3 x 10 ⁻⁴	< 2 x 10 ⁻³	< 1 x 10 ⁻³

The values in Table 14 are the values from Table 13 divided by the notional yields from Table 6. Thus the uncertainties are the combined uncertainties from those two tables.

Table 14. Fractions of Notional Yields of Combustion Products from Radiant Furnace Tests.

GAS	Initial M_{O_2}	Form	Bookcase	Sofa	Cable
CO ₂	0.21	Intact	$0.51 \pm 9\%$	$0.86 \pm 14\%$	$0.55 \pm 12\%$
	0.21	Diced	$0.53 \pm 9\%$	$0.85 \pm 11\%$	$0.54 \pm 12\%$
	0.17	Intact	$0.47 \pm 9\%$	$0.84 \pm 12\%$	$0.50 \pm 18\%$
	0.17	Diced	$0.44 \pm 9\%$	$0.82 \pm 12\%$	$0.59 \pm 12\%$
CO	0.21	Intact	$0.0168 \pm 40\%$	$0.023 \pm 36\%$	$0.044 \pm 8\%$
	0.21	Diced	$0.0158 \pm 16\%$	$0.027 \pm 19\%$	$0.050 \pm 16\%$
	0.17	Intact	$0.0154 \pm 9\%$	$0.029 \pm 18\%$	$0.047 \pm 30\%$
	0.17	Diced	$0.0200 \pm 15\%$	$0.040 \pm 30\%$	$0.055 \pm 20\%$
HCN	0.21	Intact	$< 4 \times 10^{-3}$	$< 2 \times 10^{-2}$	$0.22 \pm 70\%$
	0.21	Diced	$< 2 \times 10^{-3}$	$1.8 \times 10^{-2} \pm 50\%$	< 0.08
	0.17	Intact	$< 4 \times 10^{-3}$	$5 \times 10^{-3} \pm 75\%$	$0.012 \pm 55\%$
	0.17	Diced	$< 2 \times 10^{-3}$	$1.8 \times 10^{-2} \pm 70\%$	< 0.2
HCl	0.21	Intact	$0.1 \pm x3$	< 0.2	$0.60 \pm 35\%$
	0.21	Diced	$0.2 \pm 50\%$	$0.15 \pm 45\%$	$0.94 \pm 40\%$
	0.17	Intact	$< 8 \times 10^{-2}$	< 0.1	$0.75 \pm 40\%$
	0.17	Diced	$< 3 \times 10^{-2}$	< 0.07	$0.96 \pm 20\%$

This page intentionally left blank

V. DISCUSSION

A. Overall Test Values

The principal outcome of this series of tests is a well-documented set of combustion product yields. This includes the numerical values themselves, the apparatus conditions under which they were obtained, the uncertainty in their calculated values, and the repeatability of the tests.

Next most important is a determination of the extent to which the toxic gas yields are affected by variations in the test protocol that are reasonable in light of possible variations in combustion conditions in fires involving the intact products.

Third, it is important to evaluate the quality of the derived knowledge in the context of its intended use. The yield information would be used with a computational fire model (zone or CFD) to generate the time-dependent environment generated by a fire. Equations such as those in ISO 13571¹⁰ would then be used to assess whether the combination of occupancy design, contained combustibles, and occupant/responder characteristics lead to the desired level of life safety.

The documentation of the yields has been provided in the earlier sections. The following examines the context and quality of the results.

B. Specimen Performance and Test Repeatability

1. CO₂ and CO

There was no significant effect on the CO₂ and CO yields as a result of changing the initial oxygen volume fraction or dicing the test specimens.

For the bookcase and sofa specimens, the repeatability of the CO₂ yields was comparable to the uncertainties inherent in the volume fraction measurements. The scatter in the CO₂ yields from the cable specimens was modestly higher, probably reflective of the variable HCl yields and the role of HCl as a flame inhibitor.

The degree of repeatability in the CO yields was lower for all three types of specimens. The bookcase specimens were prone to unpredictable transition from flaming to smoldering, and some scoping tests had shown that the smoldering period generated a disproportionate yield of CO. There might have been some variability in the promptness in closing the shutter, isolating the combustion chamber from the collection chamber. This was not likely a major factor, since the uncertainties in the CO yields from the sofa and cable specimens were comparable to those for the bookcase specimens, and those two specimen types were less prone to smoldering. Another potential source of test-to-test variability was the promptness with which the test specimen was quenched with nitrogen following the closing of the shutter. This needs to be prescribed carefully in the test method, since the mass loss from the specimen could continue

after the shutter is closed and product gases were no longer being transferred to the collection chamber. However, this did not appear to be significant in this series of tests.

Taking a closer look at the extent to which replicate tests burned in a consistent manner, Figure 11 shows the resulting CO₂ and CO volume fraction profiles from four similar bookcase tests. The progress of each test has been normalized by the extent of the burn, i.e., the total mass lost from the test specimen. The justification for normalizing by the extent of burn is to depict the repeatability of the test. If profiles generally match, this indicates that the specimens burned in a consistent manner. If, on the other hand, the profiles vary widely, as they do for CO in Figure 11, this indicates a high variation from test to test.

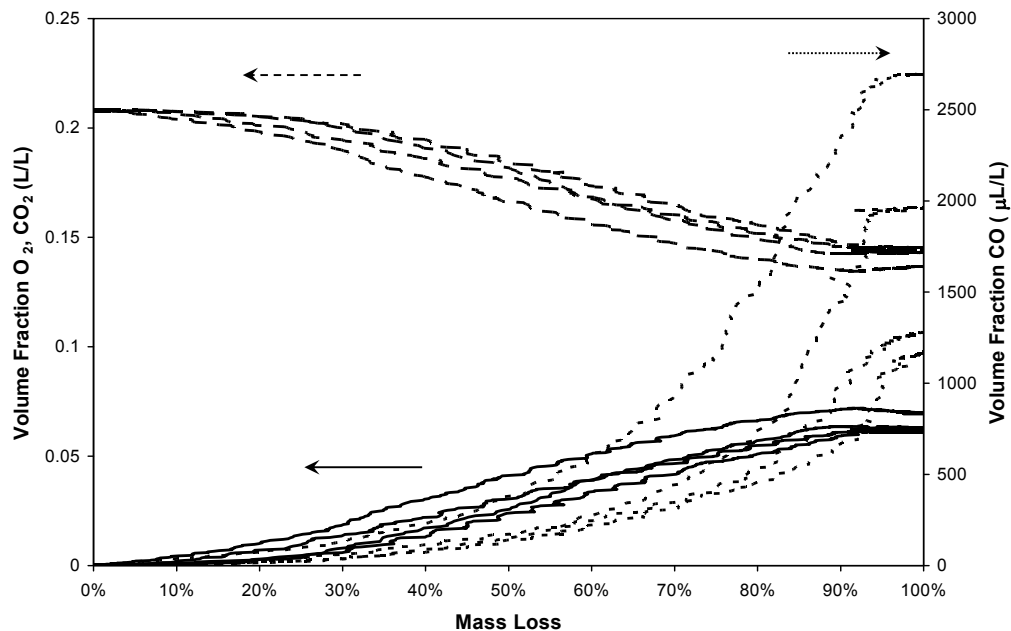


Figure 11. Gas volume fractions from four bookcase specimen tests. (Solid, CO₂; dotted, CO; dashed, O₂).

The depiction of volume fraction profiles shown in Figure 11 does not allow for easy comparison to other tests with different materials or conditions. Therefore subsequent figures show average profiles combining two or more tests of the same kind, using the following procedure. The data from a given test are rescaled so that the mass loss entries occur at regular intervals. Then, for a given mass loss percent, the volume fraction entries are averaged across multiple tests of the same type, and standard deviations taken. In the subsequent figures, the bold line represents the average of multiple tests and the lighter lines represent one standard deviation above and below that average.

So, for example, Figure 12 combines the results of four tests with an initial oxygen volume fraction of 0.21 (solid lines) to results from two tests with an initial oxygen volume fraction of 0.17 (dotted lines). Most significantly, although the oxygen volume fractions were different at

the start of the two sets of tests, by the end they were nearly the same. This implies that the particleboard burning is an oxygen-limited process and that once the oxygen volume fraction drops below ≈ 0.15 , burning in the flaming mode ceases. If flaming is limited by a lack of oxygen, then the overall effect of reducing the initial oxygen volume fraction is to reduce the overall intensity of burning—a view supported by the reduction in CO_2 production when the initial oxygen volume fraction was reduced, as seen in Figure 12.

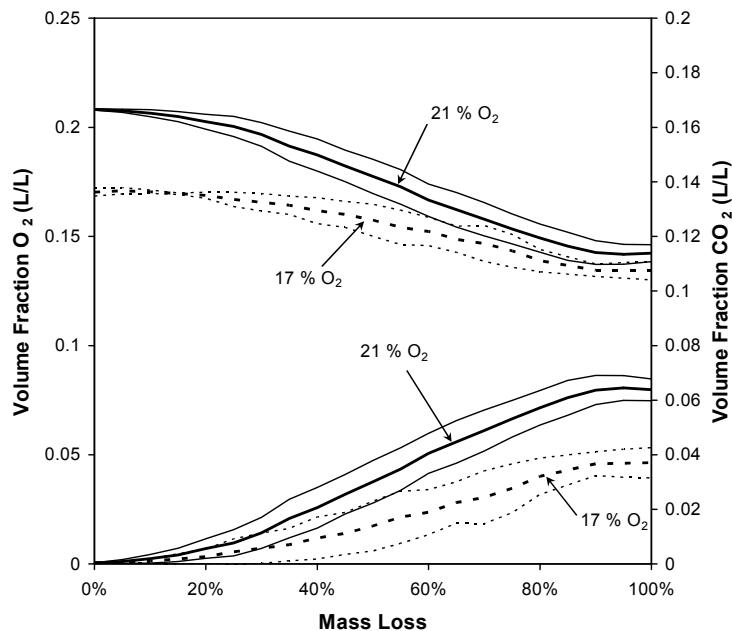


Figure 12. Comparison of oxygen consumption (top half of figure) and CO_2 production (bottom half of figure) in bookcase specimen tests at oxygen volume fractions of 0.21 (solid lines) and 0.17 (dotted lines).

The production of CO in the same sets of tests, shown in Figure 13, was also reduced when the initial oxygen volume fraction was reduced. In summary, lower initial oxygen gave less complete combustion, as expected. The difference was small, since the test specimens approached flame extinction as they approached the same residual oxygen volume fraction.

In these tests, the FED values based on the volume fractions when progress reached a mass loss of 100 percent are 0.83 and 0.74 for oxygen volume fractions of 0.21 and 0.17, respectively. (These values are slightly higher than those computed for the 30 min exposure because over the course of those 30 minutes the falling temperature of the air allows the apparatus expansion bag to deflate, which introduces air that was sequestered from the recirculating and burning process.) The change in FED is primarily the result of a reduction in CO, although the contribution from oxygen depletion actually rises slightly. These values are well in the range specified by the standard (0.5 to 1.5); if they were not, it is uncertain whether the method of adjusting the sample size would be able to compensate. If the burning of the bookcase material in this apparatus is in fact oxygen-limited, then a larger sample would experience the same absolute mass loss as a

smaller sample, in both cases burning only until the oxygen volume fraction reaches ≈ 0.14 and producing identical quantities of CO and CO₂ as were found here.

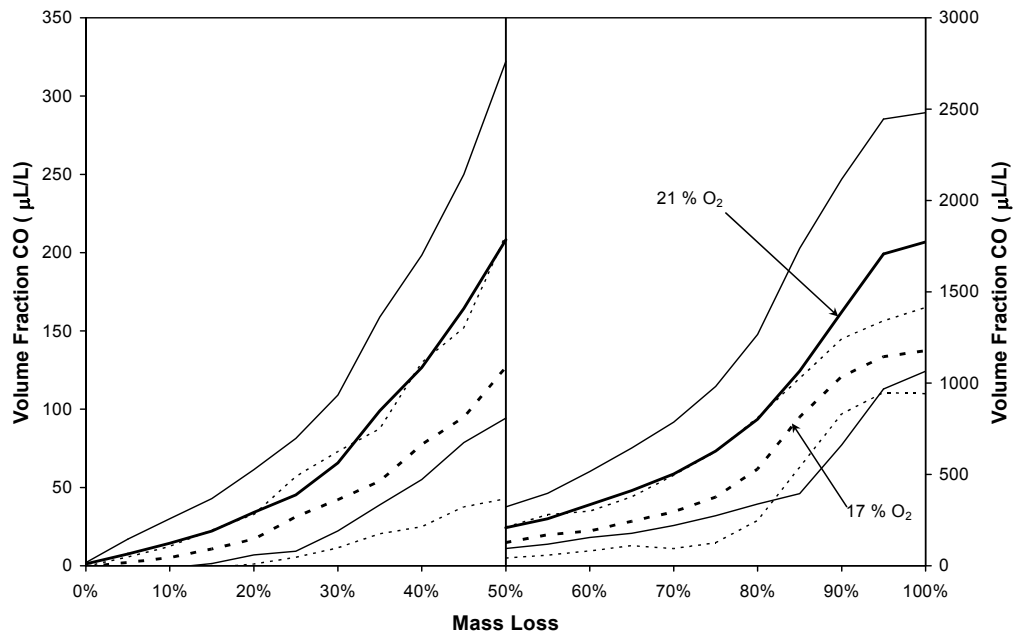


Figure 13. Comparison of CO production in bookcase specimen tests with oxygen volume fractions of 21 % (solid lines) and 17 % (dotted lines). Note the change of ordinate scale at mass loss of 50 %.

Figure 14 compares the effect of dicing the bookcase specimen, depicting the CO production as a function of mass loss fraction. The primary observation from this comparison is that dicing the material serves to reduce the scatter of the results at all stages, as indicated by the much narrower standard deviation bands. And although it appears that at earlier stages of burning the CO production was lower in the diced configuration, it ultimately reached the same value in either case. An analysis of the production of CO₂ and oxygen shows essentially the same trend - reduced scatter but ultimately reaching the same average value.

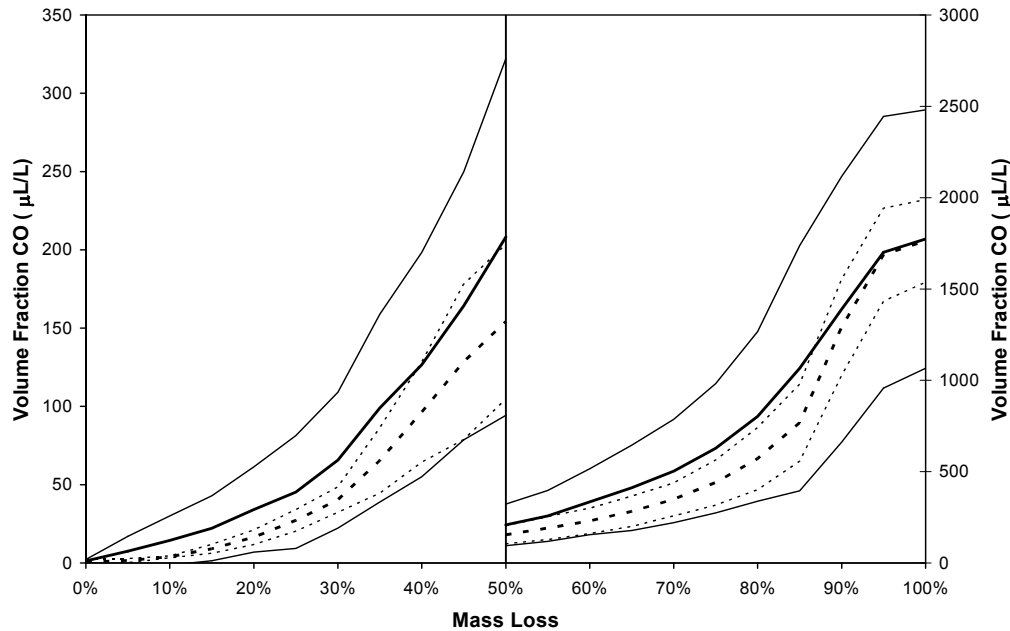


Figure 14. Comparison of CO production in bookcase specimen tests in slab (solid lines) and diced (dotted lines) configurations. Note the change of ordinate scale at mass loss of 50 percent.

Similar, but not identical behavior was found in the burning of diced and whole electrical cable specimens. As shown in Figure 15, the diced electrical cable specimens do appear to have produced less CO in the early stages of burning, but ultimately the exposure chamber CO volume fraction reached the same value as when the cables were whole. However, unlike with the bookcase specimen tests, dicing the electrical cables significantly expanded the standard deviation of the measured CO volume fractions in the later stages of burning. We hypothesize that this difference can be explained by the way dicing transformed the test specimen. In the case of the particleboard, the ignition of the whole slab depended on the behavior of the veneer, which peeled and blistered in an irregular way, changing the initial heat flux to the underlying wood. Dicing the particleboard significantly reduced the exposure of the veneer, so the primary exposure was to the homogenous wood particle matrix. The cable, on the other hand, is composed of multiple layers, including the PVC outer sheath, paper wrappers, individual conductor insulators, and the copper conductors. In the assembled product, these layers melted and burned in turn, presenting a spatially uniform material facing the radiant heaters. In the diced configuration, the cables consisted of a randomly-ordered array of 1 cm pieces of four or five different materials. This approach does not allow for strict control of the material distribution across the sample holder. Whereas dicing the bookcase material reduced its disorder to the scale of the wood particles, dicing the cable increased disorder at the 1 cm scale.

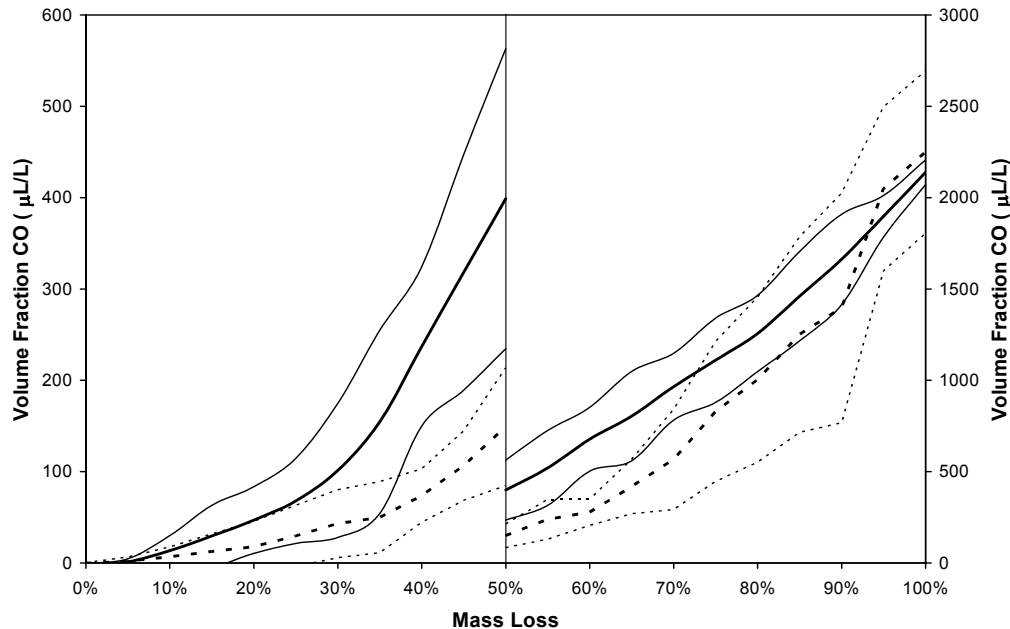


Figure 15. Comparison of CO production in electrical cable tests in whole (solid lines) and diced (dotted lines) configurations. Note the change of ordinate scale at mass loss of 50 percent.

The third set of specimens examined here, the fabric/foam combinations, was by comparison not sensitive to either configuration or initial oxygen volume fraction. Figure 16 shows the oxygen depletion and CO₂ production from tests of whole slabs of foam with initial oxygen volume fractions of 0.21 and 0.17. Unlike the bookcase tests, the sofa material tests did not appear to be limited by oxygen consumption. The oxygen depletion in either case was essentially the same. However, even in the reduced oxygen tests, the oxygen volume fraction never fell to 0.14, the limiting volume fraction for the particleboard. One reason for this low oxygen depletion was the small size of the sofa specimen (6 g compared to 90 g of bookcase material). Therefore, a larger specimen of sofa material might experience some effect from a reduced oxygen test, or if there were a larger reduction in the initial volume fraction. It should be noted that the reduced oxygen tests did have an effect on CO production, increasing its volume fraction from 500 µL/L to 750 µL/L.

Another feature of the sofa material tests was the brief duration of the flaming mode, lasting for under 1 min in most cases, compared to 2.5 min for the cable and 2 min to 5 min for the bookcase specimens. From Figure 16, it appears that both the oxygen consumption and the CO₂ generation were confined to the later stages of mass loss, behavior not seen with the other materials. We suspect that this is primarily a result of a delay on the order of 10s of seconds between the burning of the sample material, the flow of the effluent into the exposure chamber, and finally the flow to the instrument, that is masked by the longer duration of the flaming mode of the other materials. However, it is also possible that a delay exists between the gasification of the foam and the oxidation of those gases.

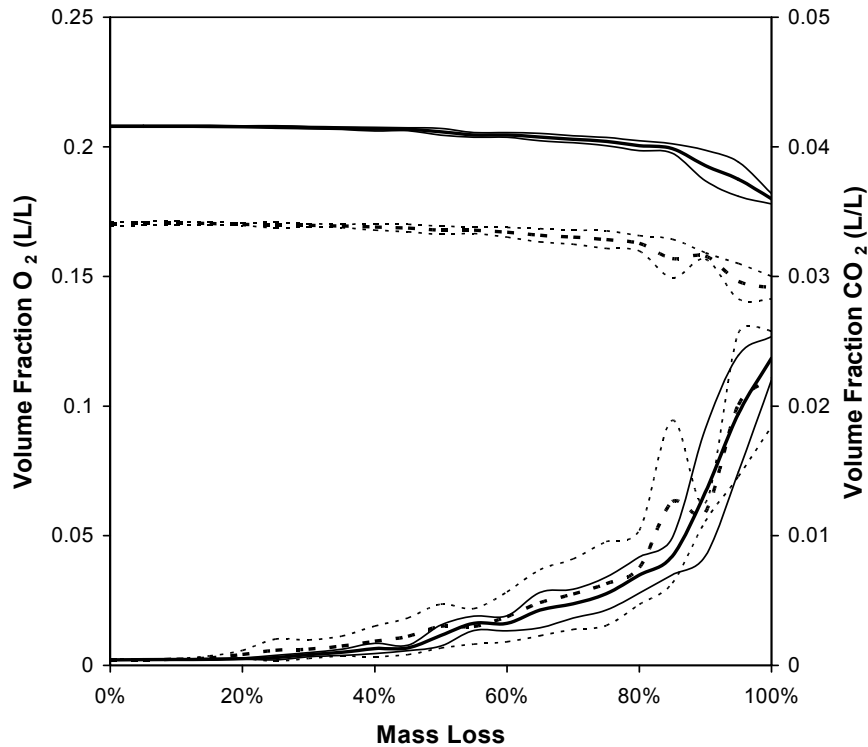


Figure 16. Comparison of oxygen consumption (top half of figure) and CO_2 production (bottom half of figure) in sofa specimen tests at oxygen volume fractions of 0.21 (solid lines) and 0.17 (dotted lines).

2. HCl and HCN

The repeatability of the HCl yields (Table 13) from the cable specimens is comparable to the CO yields, when allowing for the less precise calculation method for the HCl volume fractions. The repeatability of the HCN yields form the sofa material specimens is also reasonable, realizing that the signal-to-noise ratio was lower for this combustion product than for CO_2 , CO, or HCl.

There is a small possibility that the HCl yields from the diced cable specimens are modestly higher than from the intact specimens. Only about one-third of the combustible mass was lost during these tests, and HCl is typically generated early in the pyrolysis of PVC. Thus, exposing some of the interior PVC surface by dicing the test material might have led to increased HCl generation.

We do not find that any significant differences in HCN yield from the sofa material as a result of varying the configuration or oxygen volume fraction. It might appear that dicing the test specimens increased the HCN yield, but the yields are all close to the limit of detection and the differences should not be overinterpreted.

C. Measured vs. Notional Values

During sustained and complete combustion, the yield of CO₂ should approach its notional values, since CO₂ is a marker for combusted carbon. This was the case for the sofa specimens, where the yields were only about 15 percent below the notional values. The typical residual mass was approximately 10 percent of the initial mass, and it appeared to be carbonaceous.

For the bookcase specimens, the yield of CO₂ was about half its notional value. Only about one-third of the specimen mass was consumed, and the residue surface was a carbonaceous char.

The cable specimens also had CO₂ yields that were about half of its notional value. Only about one-third of the mass was consumed, and the residue was black and somewhat charred.

The yields of CO from all the specimens ranged from about 0.02 to 0.05, which corresponds to about 2 percent to 5 percent of their notional values. These values are consistent with relatively fuel-lean combustion²⁸ and are about five to ten times lower than the CO yields expected of postflashover fires.¹⁵

The yields of HCl from the cable specimens approach their notional values. The deficit may reflect scavenging by the calcium carbonate filler in the cable jacket.

The yields of HCl from the bookcase and sofa specimens are 10 percent or less of their notional values. Chlorine is present at well under one percent by mass in these two products, so even small wall losses in the chimney could have a large effect on the HCl reaching the sampling location.

Very little of the fuel nitrogen appears as HCN. This is as expected from fires that are fuel-lean, with the nitrogen probably appearing as molecular nitrogen or nitrogen oxides.

D. Species Sampling and Measurement

1. Species Measurement Using FTIR Spectroscopy

FTIR spectroscopic analysis of combustion products has become fairly common in fire research laboratories. However, that does not mean that its use is straightforward. The data from a recent round robin involving FTIR measurement of toxic combustion products from a standardized apparatus showed interlaboratory variations of up to an order of magnitude. There are documents under development in ISO TC92 SC1 and SC3 to standardize the implementation.

We were able to obtain usable information using this technique. There are a number of lessons emerging from this test series that can provide useful input to these efforts, such as the following:

- The application of FTIR spectroscopy to fire testing requires the constant attention of an experienced professional at a level well beyond the demands of the more traditional fire test instrumentation.

- To maximize the opportunity for obtaining time resolved concentration data, we selected a small volume cell of short optical path length and operated without a soot filter. While some cleaning was necessary, it was not a major impediment. However, the short path length did limit the sensitivity, and moderated our ability to determine toxicologically important levels of the major gases.
- For future work, a longer path length should be considered. This needs to be implemented in the context of burning times as short as one minute, which limits the residence time and flow pattern through the cell.
- The long, heated lines used here (and recommended in the SAFIR report²⁹ and ISO 19702³⁰) enabled quantitative collection of HCl, a compound that is generally regarded as difficult to determine.

2. Chimney Sampling

Some combustion products, such as CO₂ and CO, are generated in sufficient quantity and are sufficiently stable to be analyzed in the collection chamber. By contrast, the volume fractions of, e.g., the acid gases decay rapidly and must be either sampled as they are generated or their volume fractions in the collection chamber must be extrapolated back to the time when they first enter the chamber.

For the current experiments, the decision to sample combustion products from within the chimney was well intentioned, but was found to have its limitations. The principal caution arose from the flames often extending past the sampling point. As a result, the measured volume fractions were not necessarily indicative of those to which people might be exposed.

The limitations of the current location could be mitigated by several approaches, each requiring care in its implementation:

- The sampling port could be moved above the outlet of the chimney. The location would need to be above the reactive zone of the plume from any combustible. It would also have to be below the region where the gases begin to be diffused by the uncontrolled flow field in the collection chamber.
- The chimney could be lengthened such that the flames never extend beyond a sampling point located near the top of the chimney. The extent to which the hot walls influenced the yields of the toxic combustion products would need to be resolved.
- The sensitivity of the FTIR absorption cell could be improved, subject to the volumetric limitation mentioned above.
- Reducing the volume of the collection chamber could be considered. This would increase the volume fractions of the gases and improve the accuracy of any extrapolation to the time of generation. A more sophisticated correction would need to be applied to the volume fractions in order to reflect the change in molar volume resulting from the combustion process. It also appears that the volume reduction needed to obtain a large change in the volume fractions would also result in more rapid depletion of oxygen.

Since the vitiated air is recirculated into the combustion chamber, this more rapid oxygen depletion would change the timing of the specimen burning dynamics.

E. Importance of Undetected Gases

The equations in ISO 13571 include provision for additional gases to be included in estimating the time available for escape or refuge from a fire: HBr, HF, SO₂, NO₂, acrolein (C₃H₄O) and formaldehyde (H₂CO). There was no Br, F, or S in any of the products examined in this project, so the first three of these gases were not expected. The presence of the latter three was not detected, thus establishing the upper limits of their presence at the volume fractions listed in Table 5.

To put the potential contributions of the sensory irritant gases (HCl, NO₂, acrolein, and formaldehyde) in context, we use the equations in ISO 13571 for calculating the Fractional Effective Dose (FED) for the narcotic gases, CO₂ and CO, and the Fractional Effective Concentration (FEC) for the four sensory irritant gases.

The FED equation is:

$$FED = \left[\sum_{t1}^{t2} \frac{\varphi_{CO}}{35000} \Delta t + \sum_{t1}^{t2} \frac{\varphi_{HCN}^{2.36}}{1.2 \cdot 10^6} \Delta t \right] \exp\left[\frac{\varphi_{CO_2}}{5}\right],$$

where Δt is the exposure interval in minutes.

For the volume fractions measured in the chimney, for all three types of specimens, inhalation would result in incapacitation in times of the order of 5 min for the bookcase and cable specimens (mainly due to CO and CO₂), and 1 min for the sofa specimens (mainly due to HCN).

The FEC equation in ISO 13571 is:

$$FEC = \frac{\varphi_{HCl}}{F_{HCl}} + \frac{\varphi_{HBr}}{F_{HBr}} + \frac{\varphi_{HF}}{F_{HF}} + \frac{\varphi_{SO_2}}{F_{SO_2}} + \frac{\varphi_{NO_2}}{F_{NO_2}} + \frac{\varphi_{acrolein}}{F_{acrolein}} + \frac{\varphi_{formaldehyde}}{F_{formaldehyde}} + \sum \frac{\varphi_{irritant}}{F_{C_i}}$$

The FEC contributions of the four irritant gases were estimated from their volume fractions in the chimney and the incapacitating levels in ISO 13571 (F_{HCl} , etc.). The results are compiled in Table 15.

Table 15. Limits of Importance of Undetected Toxicants

	Volume fraction ($\mu\text{L/L}$)				FEC Contribution			
	HCl	NO_2	$\text{C}_3\text{H}_4\text{O}$	H_2CO	HCl	NO_2	$\text{C}_3\text{H}_4\text{O}$	H_2CO
Incapacitating level	1000	250	30	250				
Bookcase	0 to 110	< 40	< 20	< 40	0 to 0.1	< 0.2	< 0.7	< 0.2
Sofa	0 to 50	< 40	< 20	< 40	0 to 0.05	< 0.2	< 0.7	< 0.2
Cable	5000 to 14000	< 40	< 20	< 40	5 to 14	< 0.2	< 0.7	< 0.2

It stands out that the FEC contribution from acrolein is as much as two-thirds of an incapacitating level. This is because (a) the limit of detection is close to the listed incapacitating level and (b) the incapacitating level is very low. While there is agreement among experts that this value of 30 $\mu\text{L/L}$ is reasonable, there are data that suggest strongly that this is unnecessarily conservative. Kaplan and co-workers exposed individual baboons to various concentrations of acrolein in air.³¹ At the end of 5 min, each baboon was given a signal and could perform an action that led to escape from the test chamber. The baboons exposed at up to 500 $\mu\text{L/L}$ escaped and survived. Those exposed to higher levels escaped, but died later. These data suggest that people should be able to accommodate a nearly instantaneous exposure to, e.g., at least 300 $\mu\text{L/L}$ without becoming incapacitated. That would reduce the FEC contribution values in the acrolein column to < 0.1. This is consistent with Levin and coworkers, who developed extensive information on the effects of gas mixtures on rat lethality and incapacitation.³² They used those data to test whether the toxic potency of a small number of gases (not including acrolein, formaldehyde, and NO_2) could account for the lethality of the effluent from a variety of materials. Within the uncertainty in the results, $\pm 30\%$, there was no need to invoke additional toxicants.

Using this revised contribution of acrolein, the immediate bookcase-generated environment is incapacitating from narcotic gases within 5 min and is not incapacitating from the irritant gases. Thus, the contributions of the unmeasurable irritant gases do not affect the time to incapacitation. As one moves further from the burning object, the FED and FEC both decrease, and the irritant contributions become even less important.

The same analysis applies to the sofa specimens. In fact, for the highest HCN volume fractions, the FED would reach unity in as little as 5 s, making the role of the irritant gases less important. For the cable specimens, HCl dominates the FEC, and the roles of the other three irritant gases are minor.

This page intentionally left blank

VI. CONCLUSION

This paper reports toxic gas yield data for specimens cut from three complex combustibles: a bookcase, a sofa, and residential electrical power cable. The physical fire model used was the radiant apparatus from NFPA 269/ASTM E 1678. This apparatus allows the use of a test specimen that approximates the geometry and radiant exposure that might be experienced by the intact combustible in a well-ventilated flaming fire. In addition to performing the tests as prescribed in the standards, this work examined the effect of varying the initial oxygen concentration to approach an underventilated fire, and the effect of dicing the test specimens, to estimate the effect of the conformation of the test specimen.

There were two changes in all the testing. First, the shutter isolating the collection chamber from the combustion chamber/chimney was closed immediately upon cessation of flaming. In the standard operating procedure, the shutter is closed 15 min into the test. The change minimizes the contribution of non-flaming combustion to the measured combustion gas yields. Second, gas was extracted from a location in the chimney sampling for FTIR analysis. This was intended to decrease the limit of detection for trace gases.

The findings were as follows:

- For operation under the standard test procedure:
 - The CO₂ yields were quite repeatable and represented between half and 90 percent of the carbon in the test specimens. All specimens left a black residue that was presumably carbon-enriched, offering a (non-quantitative) explanation for the yields being below the notional yields.
 - The CO yields were generally of lower repeatability than the CO₂ yields.
 - The HCN yields were below the limit of detection for the bookcase specimens. Even for the sofa and cable specimens, the yields were no more than 2 percent of the notional yield, based on the conversion of fuel nitrogen.
 - The HCl volume fraction measurements were near the limit of detection for the bookcase and sofa specimens. For the cable specimens, the yields approached the notional yield and were moderately repeatable.
- Reducing the initial oxygen volume fraction to 0.17 had no significant effect on the yields of CO₂, CO, or HCl. The average HCN yield from the intact cable specimens (only) was substantially reduced.
- With the initial oxygen volume fraction of 0.21, dicing the test specimens had no significant effect on the any of gas yields, except for the HCN yield from the cable specimens, which was reduced.

With the initial oxygen volume fraction of 0.17, the only measured effects were an increase in the CO yield from dicing the bookcase specimens and an increase in HCN yield from dicing the sofa specimens. There was a noticeable difference in the time profile of CO release for the bookcase specimens. The CO yields were all substantially below the value of 0.2 found in real-scale post-flashover tests.

The combination of reducing the initial oxygen level and dicing the test specimen might have led to an increase in the HCl yield from the cable specimens.

- The yields of NO, NO₂, acrolein, and formaldehyde were all below their respective limits of detection.
- Combined, these findings indicate that there can be some sensitivity of the yields and the timing of release of the toxic gases to the combustion environment. This sensitivity is dependent on the chemistry and conformation of the test materials.
- The sensitivity of the short optical path FTIR cell limited the precision of this examination. However, there was sufficient information to assess the toxicological significance of the variations in the test procedure.
- Sampling from the chimney did improve the quantification of the trace gas volume fractions. Analysis of the results would be simplified by identifying a sampling point further downstream at which chemical reactivity of the products had been completed but before which extensive dilution had occurred.
- Calculation of the contributions of the gases to incapacitation of people who might be exposed to these environments showed:
 - For the bookcase material, incapacitation would result from inhalation of CO and CO₂.
 - For the sofa material, incapacitation would result from inhalation of HCN.
 - For the cable material, incapacitation would result from exposure to HCl.

If the CO yield were at the expected postflashover value of 0.2,

- For the bookcase material, incapacitation would result from inhalation of CO and CO₂.
- For the sofa material, incapacitation would result from inhalation of CO, HCN and CO₂.
- For the cable material, incapacitation would result from inhalation of CO and CO₂, perhaps with some contribution from exposure to HCl.

VII. ACKNOWLEDGMENTS

The authors express their appreciation to Michael Selepak for his assistance in performing the tests. David Mercier of Southwire, Inc. provided useful information on the formulation of the cable. Schwartzkopf Laboratories performed the elemental and thermal analyses of the combustibles.

This page intentionally left blank

REFERENCES

1. Phillips, W.G.B., Beller, D.K., and Fahy, R.F., "Computer Simulation for Fire Protection Engineering," Chapter 5-9 in *SFPE Handbook of Fire Protection Engineering*, 4th Edition, P.J. DiNenno *et al.*, eds., NFPA International, Quincy, MA, 2008.
2. http://www.nist.gov/el/fire_research/cfast.cfm.
3. Peacock, R. D., Jones, W. W., and Reneke, P. A., "CFAST – Consolidated Model of Fire Growth and Smoke Transport (Version 6): Software Development and Evaluation Guide," Natl. Inst. Stand. Technol., Special Publication 1086, (2013)
4. Peacock, R.D., Jones, W.W., and Bukowski, R.W., "Verification of a Model of Fire and Smoke Transport," *Fire Safety Journal* **21**, 89-129, (1993).
5. <http://fire.nist.gov/fds>.
6. "Fire Dynamics Simulator (Version 5): Technical Reference Guide," 4 volumes, NIST Special Publication 1018-5; National Institute of Standards and Technology, Gaithersburg, MD, (2010).
7. "Standard Test Method for Heat and Visible Smoke Release Rates for Materials and Products Using an Oxygen Consumption Calorimeter," ASTM E1354-04a, ASTM International, West Conshohocken, PA, 2004.
8. See, *e.g.*, "Standard for the Flammability (Open Flame) of Mattress Sets," 16 CFR Part 1633, *Federal Register* **70** (50), 13471-13523, 2006.
9. http://www.iso.org/iso/iso_catalogue/catalogue_tc/catalogue_tc_browse.htm?commid=50540&published=on&development=on.
10. "Life-threatening Components of Fire – Guidelines for the Estimation of Time to Compromised Tenability in Fires," ISO 13571, International Standards Organization, Geneva, 2012.
11. "Guidelines for Assessing the Fire Threat to People," ISO 19706, International Standards Organization, Geneva, 2011.
12. Gann, R.G., Babrauskas, V., Peacock, R.D., and Hall, Jr., J.R., "Fire Conditions for Smoke Toxicity Measurement," *Fire and Materials* **18**, 193-199 (1994).
13. "Guidance for Comparison of Toxic Gas Data between Different Physical Fire Models and Scales," ISO 29903, International Standards Organization, Geneva, 2012.
14. "Standard Test Method for Developing Toxic Potency Data for Use in Fire Hazard Modeling," NFPA 269, NFPA International, Quincy, MA, 2012.
15. "Standard Test Method for Measuring Smoke Toxicity for Use in Fire Hazard Analysis," ASTM E1678-10, ASTM International, West Conshohocken, PA, 2010.
16. (a) Gann, R.G., Averill, J.D., Nyden, M.R., Johnsson, E.L., and Peacock, R.D., "Smoke Component Yields from Room-scale Fire Tests," NIST Technical Note 1453, National Institute of Standards and Technology, Gaithersburg, MD, 159 pages (2003).
(b) Gann, R.G., Averill, J.D., Nyden, M.R., Johnsson, E.L., and Peacock, R.D., "Fire Effluent

- Component Yields from Room-scale Fire Tests," *Fire and Materials* **34**, 285-314, (2010), DOI: 10.1002/fam.1024.
17. Ohlemiller, T.J., and Villa, K., "Furniture Flammability: An Investigation of the California Bulletin 133 Test. Part II: Characterization of the Ignition Source and a Comparable Gas Burner," NISTIR 4348, National Institute of Standards and Technology, Gaithersburg, MD, 1990.
 18. Levin, B. C.; Braun, E.; Navarro, M.; Paabo, M., "Further Development of the N-Gas Mathematical Model: An Approach for Predicting the Toxic Potency of Complex Combustion Mixtures, in Nelson, G. L., ed., *Fire and Polymers II: Materials and Tests for Hazard Prevention*, ACS Symposium Series No. 599, pp. 293-311, American Chemical Society, Washington, DC, 1995.
 19. Kaplan, H.L., Grand, A.F., and Hartzell, G.E., *Combustion Toxicology: Principles and Test Methods*, Technology Publishing Co., Lancaster, PA, 1983.
 20. "Guidance for Evaluating the Validity of Physical Fire Models for Obtaining Fire Effluent Toxicity Data for Use in Fire Hazard and Risk Assessment – Part 2: Evaluation of Individual Physical Fire Models," ISO/TR 16312-2, International Standards Organization, Geneva, 2007.
 21. "Controlled Equivalence Ratio Method for the Determination of the Hazardous Components of Fire Effluent," ISO/TS 19700, International Standards Organization, 2010.
 22. "Reaction-to-fire Tests – Heat Release, Smoke Production, and Mass Loss Rates – Part 1: Heat Release (Cone Calorimeter Method)," ISO 5660-1, International Standards Organization, Geneva, 2002.
 23. "Plastics — Smoke Generation — Part 2: Determination of Optical Density by a Single-chamber Test, ISO 5659-2, International Standards Organization, Geneva, 1994.
 24. Babrauskas, V., Harris, Jr., R.H., Braun, E., Levin, B.C., Paabo, M., and Gann, R.G., "The Role of Bench-Scale Test Data in Assessing Real-Scale Fire Toxicity," Technical Note 1284, National Institute of Standards and Technology, 1991.
 25. Haaland, D.M.; Easterling, R.G.; and Vopicka, D.A., "Multivariate Least-Squares Methods Applied to the Quantitative Spectral Analysis of Multicomponent Samples" *Applied Spectroscopy* **39**, 73-84, (1985), doi:10.1366/0003702854249376.
 26. *Gas Phase Infrared Spectral Standards, Revision B*, Midac Corp.; Irvine, CA (1999).
 27. Speitel, L.C., "Fourier Transform Infrared Analysis of Combustion Gases," Federal Aviation Administration Report DOT/FAA/AR-01/88, 2001.
 28. Pitts, W.M., "The Global Equivalence Ratio Concept and the Formation Mechanisms of Carbon Monoxide in Fires," *Progress in Energy and Combustion Science* **21**, 197-237, (1995).
 29. "Smoke Gas Analysis by Fourier Transform Infrared Analysis,: The SAFIR Project," VTT Research Note, Technical Research Centre of Finland, 81 Pages, 1999.

30. "Toxicity testing of fire effluents -- Guidance for analysis of gases and vapours in fire effluents using FTIR gas analysis" ISO 19702, International Standards Organization, Geneva, 2006.
31. Kaplan, H.L., Grand, A.F., Switzer, W.G., Mitchell, D.S., Rogers, W.R., and Hartzell, G.E., "Effects of Combustion Gases on Escape Performance of the Baboon and the Rat," *Journal of Fire Sciences* **3**, 228-244, (1985).
32. Levin, B. C.; Braun, E.; Navarro, M.; Paabo, M., "Further Development of the N-Gas Mathematical Model: An Approach for Predicting the Toxic Potency of Complex Combustion Mixtures," American Chemical Society. Fire and Polymers II: Materials and Tests for Hazard Prevention. National Meeting, 208th. Chapter 20. ACS Symposium Series No. 599. August 21-26, 1994, Washington, DC, American Chemical Society, Washington, DC, Nelson, G. L., Editor, pp. 293-311, 1995.